

Nonzero angular momentum states of the helium atom in a strong magnetic field

W.Becken and P.Schmelcher
 Theoretische Chemie
 Physikalisch-Chemisches Institut
 Im Neuenheimer Feld 229
 69120 Heidelberg
 Federal Republic of Germany

Abstract

The electronic structure of the helium atom in the magnetic field regime $B = 0 - 100 a.u.$ is investigated, using a full configuration interaction approach which is based on a nonlinearly optimized anisotropic Gaussian basis set of one-particle functions. The corresponding generalized eigenvalue problem is solved for the magnetic quantum number $M = -1$ and for both even and odd z -parity as well as singlet and triplet spin symmetry. Accurate total electronic energies of the ground state and the first four excitations in each subspace as well as their one-electron ionization energies are presented as a function of the magnetic field. Additionally we present energies for electromagnetic transitions within the $M = -1$ subspace and between the $M = -1$ subspace and the $M = 0$ subspace treated in a previous work. A complete table of wavelengths and field strengths for the detected stationary points is given.

1 Introduction

Motivated by the astrophysical discovery of strong magnetic fields on the surfaces of white dwarfs ($\leq 10^5$ Tesla) and neutron stars ($\approx 10^8$ Tesla), the behaviour and the properties of matter in strong magnetic fields has increasingly attracted interest. The theoretical description of atoms in strong magnetic fields is well covered in the literature only for the case of the hydrogen atom (see refs.[1–7] and refs. therein). Until recently our knowledge about atoms with more than one electron in a strong magnetic field has been relatively sparse and definitely not sufficient for a comparison of the corresponding theoretical data with the mysterious absorption edges [8–10] in the spectrum of the magnetic white dwarf GD229. Those have for the

first time been identified as helium lines by Jordan *et al* [11] in 1998. This overwhelming evidence was based on results of highly accurate *ab initio* calculations performed by Becken and Schmelcher in 1998, a part of which has been published in ref.[12]. For a more detailed overview over the various theoretical approaches to the helium atom in a strong magnetic field and the corresponding literature before 1998 we refer the reader to [12] and in particular the references therein. In [12] a fully correlated configuration interaction approach has been applied to the helium atom in a strong magnetic field. Total energies for spin singlet and triplet states for both positive and negative z -parity in the subspace of vanishing magnetic quantum number $M = 0$ have been provided, thereby covering the regime of magnetic fields strengths from $B = 0$ to $B = 100a.u.$ ($B = 1a.u.$ corresponds to $2.35 \cdot 10^5$ Tesla). Additionally all the transition energies within the $M = 0$ subspace have been presented and discussed there, including the stationary components with respect to the field dependence which have been the key tool for the comparison with the observed spectra [11].

The aim of the present paper is to provide important data for states with the magnetic quantum number $M = -1$. Some data for states with positive z -parity and $M = -1$ have already successfully been used for a comparison with the astronomical observation (in [11], we used the corresponding stationary transitions in a certain field and wavelength regime). The *complete* data are presented here for the first time. Data resulting from states with negative z -parity are very recent results. The latter further extend our knowledge on the helium atom in a strong magnetic field and permit to investigate additional transitions.

For the case of triplet spin symmetry, Jones *et al* [13] very recently used a released-phase quantum Monte Carlo method for calculating accurate data. However, they cover only three field strengths, investigate less excited states for common symmetries and do not study the spin singlet states at all. Nevertheless for the common values of the field strength they confirm our data to several digits. In contrast to this the energies presented by Scrinzi [14], though in principle variational, are in the presence of a magnetic field significantly lower than ours. Carefully comparing the energies, it appears to us that they are systematically too low, i.e. most probably due to a numerical error.

We remark that performing calculations for finite magnetic quantum numbers requires within our approach drastically improved computational techniques (in comparison to the case $M = 0$) for keeping the CPU time affordable. A summary of these techniques is provided in the appendix of the present paper.

The starting point of the present paper is the nonrelativistic Hamiltonian of the helium atom with infinite nuclear mass in a magnetic field as given in section 2. To be self-contained we briefly discuss the Hamiltonian's symmetries and provide a description of the basis set as well as the full configuration interaction approach (for more details see ref.[12]). We introduce a maximal set of conserved quantities, chosen to be the total spin S^2 , the z -component S_z of the total spin, the total spatial magnetic quantum number M and the total spatial z -parity Π_z . These symmetries serve for classifying the results for the energies for $M = -1$ in sec.3. In each of the two subspaces for positive and negative z -parity we present the total energies and the ionization energies of the ground state and the first four excited states for singlet and

triplet spin symmetry. Additionally we consider in sec.3 all the transitions within the $M = -1$ subspace as well as all the possible transitions between the $M = -1$ states treated in the present paper and the $M = 0$ states given in ref.[12]. The wavelengths of all the stationary components are provided, being the basic ingredient for the successful comparison of theoretical data with the spectrum of magnetic white dwarfs in general and specifically for GD229.

2 Hamiltonian, Symmetries and basis sets

2.1 Hamiltonian and Symmetries

Assuming the magnetic field to point in the $+z$ -direction, the Hamiltonian reads

$$H = \sum_{i=1}^2 \left(\frac{1}{2} \mathbf{p}_i^2 + \frac{1}{2} B l_{zi} + \frac{B^2}{8} (x_i^2 + y_i^2) - \frac{2}{|\mathbf{r}_i|} + B s_{zi} \right) + \frac{1}{|\mathbf{r}_2 - \mathbf{r}_1|} \quad (1)$$

The one-particle operators in eq.(1) are the Coulomb potential energies $-\frac{2}{|\mathbf{r}_i|}$ of the electrons in the field of the nucleus as well as their kinetic energies, here splitted into the parts $\frac{1}{2} \mathbf{p}_i^2$, the Zeeman terms $\frac{1}{2} B l_{zi}$, the diamagnetic terms $\frac{B^2}{8} (x_i^2 + y_i^2)$ and their spin energies $B s_{zi}$. The electron-electron repulsion energy is represented by the two-particle operator $\frac{1}{|\mathbf{r}_2 - \mathbf{r}_1|}$. We remark that we use an electron spin g -factor equal 2, and any more accurate value for it can be simply incorporated by shifting the final total energies correspondingly. For remarks on the influence of relativistic effects and on a scaling relation taking into account the finite nuclear mass we refer the reader to ref.[6, 12, 15].

Analogously to ref.[12], we exploit that there exist four independent commuting conserved quantities: the total spin \mathbf{S}^2 , the z -component S_z of the total spin, the z -component L_z of the total angular momentum and the total spatial z -parity Π_z .

2.2 Basis sets

For constructing a two-particle basis set of eigenfunctions of the above mentioned conserved quantities, our central ingredient is an anisotropic Gaussian basis set of one-particle functions

$$\Phi_i(\rho, \varphi, z) = \rho^{n_{\rho i}} z^{n_{zi}} e^{-\alpha_i \rho^2 - \beta_i z^2} e^{im_i \varphi} \quad i = 1, \dots, n \quad , \quad (2)$$

which are themselves eigenfunctions of the corresponding one-particle operators of the mentioned conserved quantities. The parameters $n_{\rho i}$ and n_{zi} are restricted by

$$n_{\rho i} = |m_i| + 2k_i ; \quad k_i = 0, 1, 2, \dots \quad \text{with} \quad m_i = \dots - 2, -1, 0, 1, 2, \dots \quad (3)$$

$$n_{zi} = \pi_{zi} + 2l_i ; \quad l_i = 0, 1, 2, \dots \quad \text{with} \quad \pi_{zi} = 0, 1 \quad (4)$$

whereas the nonlinear variational parameters α_i and β_i are positive and have to be nonlinearly optimized for each field strength as described in ref.[12]. For each one-particle subspace of given symmetry we used an algorithm for determining the nonlinear parameters α_i and β_i such that the states of the hydrogen atom or the He^+ ion for that symmetry were optimally described. We emphasize that this procedure gives rise to considerable effort since it has to be repeated for each field strength separately.

We construct a basis set of spatial two-particle states by

$$|\psi_q\rangle := b_i^\dagger b_j^\dagger |0\rangle \quad i = 1, \dots, n \quad , \quad j = i, \dots, n \quad , \quad (5)$$

where b_i^\dagger is the creation operator of the i -th one-particle state $|i\rangle = b_i^\dagger |0\rangle$ whose position representation is given by eq.(2). The spin space is spanned by spin singlet or spin triplet states, and therefore the operators b_i^\dagger have to be chosen bosonic or fermionic, respectively. Selecting combinations with

$$m_i + m_j = M \quad , \quad \text{mod}(\pi_{zi} + \pi_{zj}, 2) = \Pi_z \quad , \quad (6)$$

we achieve the two-particle states (5) to be a basis set within the subspace for given total symmetries M and Π_z . The number N of two-particle basis states is thus in general smaller than $n(n+1)/2$.

We perform a **full Configuration Interaction (full CI)** approach by representing the Hamiltonian in a basis whose spatial part is given by the in general nonorthonormal states (5). Since the spin part $B \sum s_{zi}$ of the Hamiltonian can trivially be taken into account by a shift of the energies it is sufficient to represent the spatial part of the Hamiltonian H and the overlap S by

$$S_{pq} = \langle \psi_p | \psi_q \rangle \quad , \quad H_{pq} = \langle \psi_p | H | \psi_q \rangle \quad (7)$$

The matrices S and H are Hermitian, and the overlap S is additionally positive definite. Furthermore the matrix elements turn out to be real. The finite-dimensional generalized real-symmetric eigenvalue problem

$$(\underline{\underline{H}} - E \underline{\underline{S}}) \cdot \underline{\underline{c}} = 0 \quad (8)$$

provides eigenvalues E which are variational upper bounds to the exact eigenvalues of the Hamiltonian (1) within each subspace of given M and Π_z .

2.3 Matrix elements

For calculating the matrix elements of the spatial part of the Hamiltonian (1), we rewrite the former in second quantization, $\hat{H} = \hat{H}_I + \hat{H}_{II}$, where \hat{H}_I and \hat{H}_{II} denote the second-quantized counterparts of the familiar one- and two-particle operators whose position representations read

$$H_I(\mathbf{p}, \mathbf{r}) = \frac{1}{2} \mathbf{p}^2 + \frac{1}{2} \mathbf{B} \cdot \mathbf{l} + \frac{1}{8} B^2 (x^2 + y^2) - \frac{2}{|\mathbf{r}|} \quad H_{II}(\mathbf{r}_1, \mathbf{r}_2) = \frac{1}{|\mathbf{r}_2 - \mathbf{r}_1|} \quad (9)$$

Now, with $|\psi_q\rangle := b_i^\dagger b_j^\dagger |0\rangle$ and $|\psi_p\rangle := b_k^\dagger b_l^\dagger |0\rangle$ a straightforward calculation leads to

$$\langle \psi_p | \psi_q \rangle = \langle i|k\rangle \langle j|l\rangle \pm \langle i|l\rangle \langle j|k\rangle \quad (10)$$

$$\begin{aligned} \langle \psi_p | \hat{H}_I | \psi_q \rangle &= \langle i|H_I|k\rangle \langle j|l\rangle \pm \langle i|H_I|l\rangle \langle j|k\rangle \\ &\quad + \langle j|H_I|l\rangle \langle i|k\rangle \pm \langle j|H_I|k\rangle \langle i|l\rangle \end{aligned} \quad (11)$$

$$\langle \psi_p | \hat{H}_{II} | \psi_q \rangle = \langle ij|H_{II}|kl\rangle \pm \langle ij|H_{II}|lk\rangle, \quad (12)$$

where $|ij\rangle := |i\rangle \otimes |j\rangle$ and where the sign ' \pm ' stands for '+' in the singlet case and for '-' in the triplet case.

For the relatively simple evaluation of the $n(n+1)/2$ different one-particle overlaps $\langle i|k\rangle$ and matrix elements $\langle i|H_I|k\rangle$ we refer the reader to appendices A,B in ref.[12]. The two-particle matrix elements $\langle ij|H_{II}|kl\rangle$ are by no means trivial, in particular in view of the fact that their accurate and fast evaluation is necessary in order to build up the Hamiltonian matrix in an affordable amount of CPU time. In ref.[12] we discussed a method using a decomposition in Cartesian coordinates which expresses the two-particle matrix elements in series of hypergeometric functions whose evaluation has been performed by highly efficient analytical continuation formulas. The latter are necessary in order to keep the CPU time acceptable since the number of different two-particle matrix elements is of the order $N(N+1)/2$ rather than $n(n+1)/2$. However, the Cartesian decomposition becomes more and more inefficient with increasing magnetic quantum number, which is already relevant for calculations of the subspace $M = -1$. Therefore we have developped a drastically improved procedure using cylindrical coordinates which leads to an enormous gain of speed such that the computation of the whole Hamiltonian matrix becomes even faster than its diagonalization by standard library routines. The derivation of the corresponding powerful formula for the electron-electron integral is rather lengthy and complicated: we therefore present only major steps of it in appendices A,B,C of the present paper.

3 Results and discussion

Throughout the paper we use the notation $\nu_{S_z}^{2S+1} M^{(-1)^{\Pi_z}}$ for a state with spin multiplicity $(2S+1)$ and degree of excitation $\nu = 1, 2, 3, \dots$ within the subspace of given magnetic quantum number M and z -parity Π_z . The index S_z will be omitted in obvious cases. The present paper is concerned with the subspaces $^1(-1)^+$, $^3(-1)^+$, $^1(-1)^-$, $^3(-1)^-$. The correspondence between our field notation and the common spectroscopic notation $n_{S_z}^{2S+1} L_M$ in field-free space is discussed in ref.[12] (see table 1 therein). For completeness we mention that the $5^1(\pm 1)^-$ states correspond to the $6^1 D_{\pm 1}$ states whose field free energy is $-2.138982274 a.u.$, and analogously the $5^3(\pm 1)^-$ states correspond to the $6^3 D_{\pm 1}$ states with a field free energy of $-2.013901415 a.u.$ (Both values are taken from ref.[16]).

3.1 Aspects for the selection of basis functions

For the $M = 0$ states treated in ref.[12], we have been able to achieve a considerable accuracy by choosing basis sets which can describe the shape of the exact wave function, i.e. include electronic correlation effects. The latter become less important with increasing quantum number $|M|$, and this manifests itself already for $M = -1$. The reason is that bound two-particle states with nonzero values of M are approximately one-particle excitations. Consequently, the electrons are spatially more separated than in a 0^+ state, and this lowers the correlation energy. Additionally, the cusp problem is also less important for excited states $M = -1$, and therefore fewer one-particle functions with large values for the nonlinear α and β parameters are needed. We have exploited these facts and achieved even more accurate results for the $M = -1$ states than for the $M = 0$ states.

In detail the strategy was similar to the $M = 0$ case. In the case of the $(-1)^+$ subspace we used 260 optimized one-particle basis functions (for each field strength) for constructing a two-particle basis set of dimension $N = 3793$. The latter number is identical for the singlet and the triplet subspace since it cannot occur that a two-particle state contains two identical one-particle contributions which combine to the odd total magnetic quantum number $M = -1$. This is a principal difference to the case of the 0^+ subspace. In order to describe angular correlation, we have added also $(-2)^+$ and $(-3)^+$ functions which are paired with $(+1)^+$ and $(+2)^+$ functions, respectively, to build up $M = -1$. The same scheme was used for the contributions of one-particle functions of negative z -parities. There it was sufficient to use the combinations $(-1)^-/0^-$ and $(-2)^-/(-1)^-$. In order to describe excitations we added one-particle basis functions with quantum numbers $m^{\pi_z} = (-1)^+$ and values $l_i = 1$ and $k_i = 1$ (see eqs.(3,4)). The latter have exclusively been optimized for a nuclear charge number $Z = 1$, in contrast to all the other types of basis functions which have been optimized for $Z = 1$ (hydrogen) and for $Z = 2$ (He^+). The reason is again that all bound $M = -1$ states are one-particle excitations in which the excited electron is associated to the one-particle quantum numbers $m^{\pi_z} = (-1)^+$, and the effect of the nucleus on that outer electron is screened by the inner one, thereby giving rise to an effective nuclear charge close to unity.

For the $(-1)^-$ subspace we proceeded in a similar manner, the basis set dimension was $N = 3671$ for both singlet and triplet states, built up from a set of 228 optimized one-particle basis functions of type (2).

In the following, we present and discuss the results for the helium energy calculations. Comparing our field-free data with the literature we observe that they are for the subspace $(-1)^+/(-1)^-$ subspaces more accurate than in the case of the $0^+/0^-$ subspaces. We will as far as possible compare our helium energies for finite field strength with the best data available in the literature.

3.2 Energies for finite field strengths

3.2.1 Results for $M = -1$ and even z -parity

a) The singlet states $\nu^1(-1)^+$

For the singlet subspace $\nu^1(-1)^+$ we present the energies of the ground state and the first four excitations, i.e. $1 \leq \nu \leq 5$. The energies for the $1^1(-1)^+$ state are presented in table 1, together with the values given in the literature, if available. The accuracy of the field free energy is even higher than the ones of the $1^1 0^+$ and $1^1 0^-$ states due to the lower correlation energy for the $M = -1$ states. We remark that even though the data for the $(-1)^+$ symmetry presented in ref.[11] have been accurate enough for identifying features in the spectrum of the magnetic white dwarf GD229 as absorption edges of helium, we have been able to improve the accuracy slightly.

We observe that for small values of B the total energies of the $1^1(-1)^+$ state lie slightly lower than for $B = 0$ which is an effect due to the Zeeman energy which is negative for $M = -1$. However, for fields stronger than $B \approx 0.16 a.u.$ the total energies rise drastically with increasing field strength which has its origin in the increasing kinetic energy of the electrons which can roughly be estimated by their Landau energy amounting to B for both electrons together.

In order to reveal the internal energetics of the atom we have to subtract such pure and overall field effects. For an analysis it is advantageous to subtract even more: one measure for the accuracy of the total energies $E(B)$ are their corresponding one-particle ionization energies $|E(B) - T(B)|$ corresponding to the process $\text{He} \rightarrow \text{He}^+ + e^-$. The threshold $T(B)$, i.e. the lowest possible total energy for which the system $\text{He}^+ + e^-$ can exist possessing the *same* quantum numbers as the He state in question, is given in the fourth column in table 1 (the values for the ionization energies are trivial to compute and are not additionally listed in any of the tables). The values $T(B)$ for $(-1)^+$ symmetry are identical to those given in ref.[12] for the $M = 0$ symmetry. The reason is that for any z -parity and spin symmetry the lowest $M = -1$ state of the system $\text{He}^+ + e^-$ is realized by the ionized electron in a Landau state with magnetic quantum number $m = -1$ and the He^+ ion in its 0^+ ground state: the Landau energy of the electron depends on $(m + |m|)$ and is therefore identical for $m = -1$ and $m = 0$. The alternative possibility of associating the value $m = -1$ to the He^+ ion possesses a higher energy.

The energies for the excited states $\nu^1(-1)^+$, $2 \leq \nu \leq 5$ are given in table 2. We remark that for finite field strengths there are no data about these states available in the literature so far. We observe as expected that their total energies rapidly approach the threshold $T(B)$ with increasing excitation.

The dependence of the one-particle ionization energies on the field strength is shown in figure 1. In contrast to the total energies of the $1^1(-1)^+$ state its ionization energy depends monotonously on B : the outer electron becomes increasingly bound with increasing field strength. This is not in general the case for the excited states within the $(-1)^+$ subspace although the ionization energy of the $2^1(-1)^+$ state is monotonous (note the changes in the slope compared to the $1^1(-1)^+$ state). The ionization energies of the states $3^1(-1)^+$, $4^1(-1)^+$ and $5^1(-1)^+$ exhibit a pattern of several avoided crossings. Those occur in the

field strength interval $0.02 \leq B \leq 0.2$ which is the regime where a rearrangement takes place: for low field strengths the states $3^1(-1)^+$ and $4^1(-1)^+$ (field free 4^1F_{-1} and 4^1P_{-1}) are energetically almost degenerate since they both belong to the field free principal quantum number $n = 4$. This degeneracy is disturbed by the magnetic field and completely destroyed for strong fields (see figure 1).

b) The triplet states $\nu^3(-1)^+$

For the triplet subspace $\nu^3(-1)^+$ we present the energies for the ground state and the first four excitations, i.e. $1 \leq \nu \leq 5$. The total energies of the states with $S_z = -1$ are given in table 3 together with data existing in the literature for the states $1^3(-1)^+$, $2^3(-1)^+$ and $3^3(-1)^+$. The states $4^3(-1)^+$ and $5^3(-1)^+$ have not been present in the literature so far. We observe that our energies are variationally lower than any values in the literature apart from only a few exceptions with respect to the energies computed by Jones *et al* [13]. However, one must take into account that the released-phase quantum Monte Carlo method performed by Jones *et al* leads to statistical error bars (see the corresponding numbers in parentheses in table 3) such that none of those energies is significantly stronger bound than our results. This means, either we confirm these results or our accuracy is even higher, reflecting the fact that our optimized anisotropic Gaussian basis sets excellently describes the wave functions in a magnetic field. Due to the efficiency of our method of computation we were able to cover a large number of field strengths.

Due to the spin shift BS_z the triplet states with $S_z = -1$ are the most strongly bound ones among the three states with $S_z = 0, \pm 1$. This spin shift causes the $1^3_{-1}(-1)^+$ state to cross the low-field ground state $1^1 0^+$ at $B \approx 0.750 a.u.$ For $B \gtrsim 0.750 a.u.$ the $1^3_{-1}(-1)^+$ state is the global ground state of the atom. The $1^3_{-1}(-1)^+$ state is for any field strength lower than the $1^3_{-1}(-1)^-$ state (see sec. 3.2.2), and it lies also lower than the $1^3_{-1} 0^+$ and $1^3_{-1} 0^-$ states for $B \geq 0.750 a.u.$. The latter ones cross the $1^1 0^+$ state at $B \approx 1.112 a.u.$ and $B \approx 0.994 a.u.$, respectively.

Analogously to the singlet case, we show the one-particle ionization energies of the triplet states also in figure 1. We observe that the singlet-triplet splitting decreases with increasing excitation. This occurs due to the fact that for excitations the spatial separation between the electrons is large, and therefore the exchange terms in eqs.(10-12) are small which causes a small effect of the different signs of the matrix elements belonging to singlet and triplet states.

3.2.2 Results for $M = -1$ and odd z -parity

a) The singlet states $\nu^1(-1)^-$

For the singlet subspace $\nu^1(-1)^-$ we present also the ground state and the first four excitations, i.e. $1 \leq \nu \leq 5$. The total energies are given in table 4. Like in the case of the excited $^1(-1)^+$ states there exist no data for finite field strengths in the literature. Our field-free data are in good agreement with the literature. In figure 2 we show the one-particle ionization energies analogously to figure 1. The threshold $T(B)$ is identical to the case of $(-1)^+$, 0^+ or 0^- symmetry because the energetically lowest way to realize

the ionized system $\text{He}^+ + e^-$ with $(-1)^-$ symmetry is to leave one electron in the 0^+ state of a He atom. The other electron must then be placed in a Landau orbital with $m = -1$ and negative z -parity, which does not affect the Landau energy $B/2$.

b) The triplet states $\nu^3(-1)^-$

For the triplet states, several investigations exist in the literature [13, 18–21], in contrast to the singlet case. In table 5 we have listed our total energies and the corresponding values of the literature for the states $\nu_{-1}^3(-1)^-$ (i.e. $S_z = -1$), $1 \leq \nu \leq 5$. Again our results are better than almost all the reference values for finite field strengths or are at least comparable to the ones of Jones *et al* [13] within their statistical error bars. For the states $3^3(-1)^+$ and $4^3(-1)^+$ there exist no data in the literature so far.

In figure 2 we show the ionization energies. The dashed triplet curves almost coincide with the corresponding singlet curves. Such a small singlet-triplet splitting is in good agreement with the considerations mentioned in sec.3.2.1 which predict a small singlet-triplet splitting for high excitations.

4 Transitions

For the comparison of the energy levels of helium with the spectra of magnetic white dwarfs in general and GD229 in particular it is necessary to determine the transition energies from our total energies. Restricting ourselves to electric dipole transitions, we have the selection rules $\Delta S = 0$, $\Delta S_z = 0$ for the spin degrees of freedom in our nonrelativistic approach and $\Delta M = 0$, $\Delta \Pi_z = \pm 1$ (for linearly polarized radiation) or $\Delta M = \pm 1$, $\Delta \Pi_z = 0$ (for circularly polarized radiation) for the spatial degrees of freedom. Whereas in ref.[12] we were already able to present the $\Delta M = 0$ transitions $0^+ \leftrightarrow 0^-$, we are now able to investigate three times as many transitions: firstly the $\Delta M = 0$ transitions between the $(-1)^+$ and the $(-1)^-$ states, and additionally two classes of $|\Delta M| = 1$ transitions between the $M = -1$ states and $M = 0$ states, involving positive and negative z -parities, respectively. Altogether our data yield 75 singlet and 70 triplet transitions.

Due to the fact that the field strengths in the atmospheres of magnetic white dwarfs is not a constant but varies by a factor of two for a dipole geometry, transitions which behave monotonically as a function of the varying field are smeared out, i.e. are not expected to provide a signature in the observed spectrum. However, the transitions whose wavelengths are stationary with respect to the field dependence manifest themselves as absorption edges in the observable spectrum if they possess a relevant intensity. We therefore give in tables 6 to 11 a complete list of all the stationary points which resulted from our calculated transitions.

We remark that for a reliable comparison with observational spectra in some cases the finite nuclear mass effects have to be taken into account. This requires corrections of our total energies according to the scaling relation given in eq.(4) in ref.[12] and in refs.[6, 15]. Due the selection rules $\Delta S = 0$, $\Delta S_z = 0$, we have for the transition energies the scaling relation $\Delta E(M_0, \mu^2 B) = \mu \Delta E(\infty, B) - \frac{1}{M_0} \mu^2 B \Delta M$ (here $M_0 = 7344 a.u.$ is the nuclear mass and $\mu = 0.999864 a.u.$ is the reduced mass). For $\Delta M = 0$ transitions

the effect is always such that the position (field strength) and wavelength of a mass-corrected stationary point are related to the corresponding fixed-nucleus result by $B(M_0) = \mu^2 B(\infty)$ and $\lambda(M_0) = \frac{1}{\mu} \lambda(\infty)$. If for $|\Delta M| = 1$ transitions the ratio $\frac{B}{M_0}$ is small compared to ΔE it is still possible to do an approximate correction for the wavelengths of the stationary points directly with the data presented: We then have $\lambda(M_0) = \frac{1}{\mu} \lambda(\infty) (1 + \mu \frac{B}{M_0} \lambda(\infty) \Delta M)$. The stationary points corrected exactly within the scaling relation given above can, of course, only be obtained by separately scaling all the values of ΔE and by interpolating them over the grid of scaled field strengths. In the argumentation above we have taken into account the normal mass correction terms. The specific mass corrections are expected to be even less significant, in particular for stronger fields and excited states.

Altogether we detected 139 stationary points; several ones among them possess large uncertainties which arise mainly due to the interpolation error with respect to the crude grid of field strengths. Most of the transitions $(-1)^+ \leftrightarrow 0^+$, however, are so precise that the corresponding data have already successfully been used to explain the absorption edges in the spectrum of the white dwarf GD229[11], and these data together with the other stationary transitions serve as a good basis for astrophysicists to investigate the spectra of unidentified magnetic objects.

5 Concluding remarks and Outlook

We have investigated the fixed-nucleus electronic structure of the helium atom in a magnetic field by a fully correlated approach. Scaling laws allow to include finite-mass effects. The present work is concerned with the energy levels and transitions of the helium states with magnetic quantum number $M = -1$. A small part of the corresponding data has already been used successfully for identifying the features in the spectrum of the white dwarf GD229 with electronic transitions in atomic helium[11], which represented one of the goals of our work. The enlarged data presented in this paper will now, together with the energy levels provided in ref.[12], serve as a good starting point for the analysis of observed spectra of magnetic astrophysical objects in general.

The reliability of our wavelength data results from the high accuracy of our energy values which ranges between $10^{-4} a.u.$ and $10^{-6} a.u.$. This accuracy has become possible due to our approach by means of an optimized anisotropic Gaussian basis set. Since the spherical invariance is broken by the magnetic field, it has been necessary to use Gaussians with different length scales for the longitudinal and transversal degrees of freedom. The nonlinear parameters describing these length scales have been determined by the requirement to solve optimally the one-particle problem of the H atom or the He^+ ion in a magnetic field of given strength. These optimized one-particle functions have been used to construct configurations in order to represent the full fixed-nucleus Hamiltonian and the overlap as matrices separately in each subspace of fixed quantum numbers corresponding to the four conserved quantities: the total spin \mathbf{S}^2 and its z -component S_z ,

the z -component L_z of the electronic angular momentum and the electronic z -parity Π_z . The corresponding generalized eigenvalue problem provided a variational estimation for the energy eigenvalues.

Atomic energies of helium have been calculated for the ground state and the first four excitations in each subspace for $M = -1$, i.e. for positive and negative z -parity as well as for singlet and triplet spin symmetry. We considered altogether 20 different field strengths $0 \leq B \leq 100 a.u.$, i.e. $0 \leq B \leq 2.3505 \cdot 10^7$ Tesla. This series production of data has become by very efficient algorithms for the computation of the matrix elements, in particular the electron-electron matrix elements for which we presented an analytical formula derived in cylindrical coordinates, thereby making the CPU effort for the calculations for nonzero angular momentum affordable: Building up a matrix of dimension about 4000 takes less than one hour CPU time on a moderate Silicon Graphics workstation.

The comparison of energy data with observed spectra of astrophysical objects is possible by searching for stationary points of the transitions with respect to the magnetic field strength. The data for $M = -1$ in the present paper yield $\Delta M = 0$ transitions, and together with the results for $M = 0$ in ref.[12] we have also been able to consider $\Delta M = 1$ transitions. Complete tables of all the detected stationary points for the mentioned transitions were given. Energy data for $M = -2$ and $M = -3$ are planned to be investigated in a future work.

In order to complete the treatment of bound electronic transitions of helium in a magnetic field, we will in the near future also investigate in detail the oscillator strengths of the mentioned transitions as a function of the magnetic field. Based on the calculated intensities it will be possible to produce synthetic spectra, and a comparison with the observed spectra will give important hints for models of the radiation transport and the field configuration in magnetic astrophysical objects.

Acknowledgements. The Deutsche Studienstiftung (W.B.) and the Deutsche Forschungsgemeinschaft (W.B.) are gratefully acknowledged for financial support.

A Analytical solution to the electron-electron integral

In the following it is our aim to derive an analytical expression for the electron-electron integral which allows its efficient numerical implementation. We emphasize that an efficient treatment of the two-particle integrals is essential for the calculations on helium since the number of two-particle matrix elements is $N(N+1)/2$, in contrast to the one-particle matrix elements whose number is only $n(n+1)/2$ (here $N \approx 4000$ is the dimension of the two-particle Hamiltonian matrix whereas $n \approx 200$ is the dimension of the underlying one-particle basis set, see eqs.(2,5)). Denoting the two-particle interaction with $V_{II}(\mathbf{r}_1, \mathbf{r}_2) = \frac{1}{|\mathbf{r}_1 - \mathbf{r}_2|}$, we have to solve the integral

$$\langle ij|V_{II}|kl\rangle = \int d^3r_1 d^3r_2 \Phi_i(\mathbf{r}_1)\Phi_j(\mathbf{r}_2) \frac{1}{|\mathbf{r}_1 - \mathbf{r}_2|} \Phi_k(\mathbf{r}_1)\Phi_l(\mathbf{r}_2), \quad (\text{A.1})$$

where the one-particle orbitals Φ_i are of type (2), obeying the constraints (3,4). For the sake of brevity, we will in the following use the index notation $\gamma_{ik} := \gamma_i + \gamma_k$ for the sum of two indexed quantities.

The initial step is to apply a Singer transformation [22] in order to remove the Coulomb singularity, thereby introducing the new variable u according to $\frac{1}{|\mathbf{r}_1 - \mathbf{r}_2|} = \frac{2}{\sqrt{\pi}} \int_0^\infty du e^{-u^2(\mathbf{r}_1 - \mathbf{r}_2)^2}$. Then the integrand of this new integration over u decomposes into a transversal and a longitudinal part

$$\langle ij|V_{II}|kl\rangle = \frac{2}{\sqrt{\pi}} \int_0^\infty du I_{\rho\varphi}(u) \cdot I_z(u), \quad (\text{A.2})$$

where

$$I_z(u) = \int_{-\infty}^\infty dz_1 \int_{-\infty}^\infty dz_2 z_1^{n_{zik}} z_2^{n_{zjl}} e^{-\beta_{ik}z_1^2 - u^2(z_1 - z_2)^2 - \beta_{jl}z_2^2} \quad (\text{A.3})$$

and

$$I_{\rho\varphi}(u) = \int \rho_1 d\rho_1 d\varphi_1 \rho_2 d\rho_2 d\varphi_2 \rho_1^{n_{\rho ik}} e^{-i(m_i - m_k)\varphi_1} e^{-\alpha_{ik}\rho_1^2} \cdot e^{-u^2(\rho_1^2 + \rho_2^2 - 2\rho_1\rho_2 \cos(\varphi_2 - \varphi_1))} \quad (\text{A.4})$$

$$\times \rho_2^{n_{\rho jl}} e^{-i(m_j - m_l)\varphi_2} e^{-\alpha_{jl}\rho_2^2}$$

The longitudinal integral $I_z(u)$ is the trivial part of the matrix element (A.1). For decoupling the particles 1 and 2 we substitute $\tilde{z}_1 = z_1 - b(u)z_2$, $\tilde{z}_2 = z_2$ where $b(u) = \frac{u^2}{\beta_{ik} + u^2}$ and $\frac{\partial(\tilde{z}_1, \tilde{z}_2)}{\partial(z_1, z_2)} = 1$. The exponential factorizes, and the power $z_1^{n_{zik}}$ can be multiplied out, yielding for $I_z(u)$ a sum over standard integrals of the Gaussian type $\int_{-\infty}^\infty z^{n_z} e^{-\gamma(u)z^2}$ which can easily be evaluated, giving after a few steps of algebra

$$I_z(u) = 4g_{n_{zijkl}} \sum_{\zeta=0}^{\zeta \leq \frac{n_{zik}}{2}} \binom{n_{zik}}{2\zeta} J(n_{zik}, n_{zjl}, \beta_{ik}, \beta_{jl}; 2\zeta; u) \quad (\text{A.5})$$

where the prefactor $g_l := \text{mod}(l, 2)$ reflects the fact that the total z -parity is a conserved quantity. The function J is defined by

$$J(n_1, n_2, a_1, a_2; v; u) = \frac{1}{4} a_1^{-n_1 - \frac{1}{2}} a_2^{-\frac{n_{12}+1}{2}} \cdot \Gamma\left(\frac{v+1}{2}\right) \cdot \Gamma\left(\frac{n_1+n_2-v+1}{2}\right) \cdot (a_1 a_2)^{\frac{v}{2}} \quad (\text{A.6})$$

$$\times u^{2(n_1-v)} \left(1 + \frac{1}{a_1} u^2\right)^{\frac{n_2-n_1}{2}} \left(1 + \frac{a_{12}}{a_1 a_2} u^2\right)^{-\frac{n_{12}-v+1}{2}}$$

The usual procedure for the treatment of the transversal part $I_{\rho\varphi}$ would be to represent it in Cartesian coordinates since then its decomposition into a sum of products of integrals $I_x(u)$ and $I_y(u)$ analogous to $I_z(u)$ would be technically simple: The exponential would factorize automatically, and the remaining part consists of factors like $\rho^{n_\rho} e^{\pm i m}$ which can be expressed as $(x^2 + y^2)^k (x \pm i y)^{|m|}$ due to the constraint (3) and which can trivially be multiplied out. We emphasize that this procedure, however, would yield expressions which are very expensive with respect to the CPU time since already for small nonzero magnetic quantum numbers m or excitations k the number of binomic terms gives rise to a large number of integrals over u .

In the following we exploit that the described drawback is not at all a property of the integral (A.1) but only of the Cartesian approach. In fact, the many mentioned u -integrals are not independent from each other but the information how to resummize their results to a more compact expression is lost in the lengthy Cartesian algebra. Therefore, it is our strategy to use cylindrical coordinates from the very beginning, although the derivation of this condensed analytical formula is technically involved.

The key for solving the integral $I_{\rho\varphi}(u)$ is the following substitution

$$\tilde{\rho}_1 = \sqrt{\rho_1^2 + a^2 \rho_2^2 - 2a\rho_1\rho_2 \cos(\varphi_2 - \varphi_1)} \quad \tilde{\rho}_2 = \rho_2 \quad (\text{A.7})$$

$$\sin \tilde{\varphi}_1 = \frac{\rho_1}{\tilde{\rho}_1} \sin(\varphi_2 - \varphi_1); \quad \cos \tilde{\varphi}_1 = \frac{\rho_1}{\tilde{\rho}_1} \cos(\varphi_2 - \varphi_1) - a \frac{\rho_2}{\tilde{\rho}_1} \quad \tilde{\varphi}_2 = \frac{1}{2}(\varphi_2 + \varphi_1) \quad (\text{A.8})$$

which results from the following ideas (here $a(u) = \frac{u^2}{\alpha_{ik} + u^2}$). Firstly, we use the angular part of $I_{\rho\varphi}(u)$ for exploiting the conservation of L_z , and secondly the remaining radial part has to be decoupled similarly like in the case of the z -integration mentioned above. Using in eq.(A.5) the angle $\varphi := \varphi_2 - \varphi_1$ and the cyclic angle $\bar{\varphi} := \frac{1}{2}(\varphi_2 + \varphi_1)$, the integration over $\bar{\varphi}$ yields a Kronecker Delta reflecting the conservation of L_z :

$$\begin{aligned} I_{\rho\varphi}(u) &= 2\pi \delta_{m_{ij}, m_{lk}} \int_0^\infty \rho_1 d\rho_1 \int_0^\infty \rho_2 d\rho_2 \rho_1^{n_{\rho_{ik}}} e^{-\alpha_{ik}\rho_1^2} \cdot \rho_2^{n_{\rho_{jl}}} e^{-\alpha_{jl}\rho_2^2} \cdot e^{-u^2(\rho_1^2 + \rho_2^2)} \\ &\quad \times \int_0^{2\pi} d\varphi e^{i(m_i - m_k)\varphi} \cdot e^{-u^2(-2\rho_1\rho_2 \cos \varphi)} . \end{aligned} \quad (\text{A.9})$$

Now, the expression $(\rho_1 \cos \varphi)$ plays a similar role as z_1 in eq.(A.3), and therefore we temporarily introduce $\xi_1 = (\rho_1 \cos \varphi)$ and $\eta_1 = (\rho_1 \sin \varphi)$ as dummy Cartesian variables. For decoupling the particles 1 and 2 analogously to the treatment of $I_z(u)$ we substitute $\tilde{x}_1 = \xi_1 - a\tilde{\rho}_2$ whereas $\tilde{y}_1 = \eta_1$ and $\tilde{\rho}_2 = \rho_2$ remain unchanged. The variables $\tilde{\rho}_1$ and $\tilde{\varphi}_1$ given in eqs.(A.7,A.8) are now just the new cylindrical coordinates belonging to \tilde{x}_1 and \tilde{y}_1 . In this new representation $I_{\rho\varphi}$ reads

$$\begin{aligned} I_{\rho\varphi}(u) &= 2\pi \delta_{m_{ij}, m_{lk}} \int_0^{2\pi} d\tilde{\varphi}_1 \int_0^\infty d\tilde{\rho}_1 \tilde{\rho}_1 \cdot \rho_1^{n_{\rho_{ik}}} e^{-(\alpha_{ik} + u^2)\tilde{\rho}_1^2} \cdot e^{i(m_i - m_k)\varphi_1} \\ &\quad \times \int_0^\infty d\tilde{\rho}_2 \tilde{\rho}_2^{n_{\rho_{jl}} + 1} e^{-\frac{\alpha_{ik}\alpha_{jl} + \alpha_{ijkl}u^2}{\alpha_{ik} + u^2}\tilde{\rho}_2^2} , \end{aligned} \quad (\text{A.10})$$

where the variables ρ_1 and φ_1 occuring in the factor $\rho_1^{n_{\rho_{ik}}} e^{i(m_i - m_k)\varphi_1}$ have to be considered as functions of the variables labelled with the symbol (\sim) . We split $\rho_1^{n_{\rho_{ik}}} e^{i(m_i - m_k)\varphi_1} = \rho_1^{2k_{ik}} \cdot \rho_1^{|m_i| + |m_k|} e^{i(m_i - m_k)\varphi_1}$ according to eq.(3). This is a powerful step since the relations (A.7,A.8) can explicitly be solved with respect to those two factors. After some algebra we arrive at:

$$\rho_1^{2k_{ik}} = \sum_{r_1 + r_2 + r_3 + r_4 = k_{ik}} \begin{pmatrix} k_{ik} \\ r_1 \ r_2 \ r_3 \ r_4 \end{pmatrix} a^{2r_2 + r_3 + r_4} \tilde{\rho}_1^{2r_1 + r_3 + r_4} \tilde{\rho}_2^{2r_2 + r_3 + r_4} e^{i(r_3 - r_4)\tilde{\varphi}_1} \quad (\text{A.11})$$

$$\rho_1^{|m_i|+|m_k|} e^{i(m_i-m_k)\varphi_1} = \sum_{\mu_i=0}^{|m_i|} \binom{|m_i|}{\mu_i} \sum_{\mu_k=0}^{|m_k|} \binom{|m_k|}{\mu_k} a^{|m_i|+|m_k|-\mu_{ik}} \tilde{\rho}_1^{\mu_{ik}} \tilde{\rho}_2^{|m_i|+|m_k|-\mu_{ik}} e^{i(s_i\mu_i-s_k\mu_k)\varphi_1} \quad (\text{A.12})$$

where $s_i := \text{sgn}(m_i)$ are the signs of the magnetic quantum numbers. Inserting the expressions (A.11,A.12) into eq.(A.10), we can perform the $\tilde{\varphi}_1$ -integration yielding a Kronecker Delta which restricts the summation indices to $r_3-r_4 = -s_i\mu_i+s_k\mu_k$. The obtained sum is a decomposition of $I_{\rho\varphi}$ into products of each two radial Gaussian integrals completely analogous to the expressions encountered in the evaluation of the integral I_z , which allows us after several steps to express also $I_{\rho\varphi}$ in terms of the function J given in eq.(A.6):

$$I_{\rho\varphi}(u) = 4\pi^2 \delta_{m_{kl},m_{ij}} \sum_{\mu_i=0}^{|m_i|} \binom{|m_i|}{\mu_i} \sum_{\mu_k=0}^{|m_k|} \binom{|m_k|}{\mu_k} \sum_{\substack{r_1+r_2+r_3+r_4=k_{ik} \\ r_3-r_4=-s_i\mu_i+s_k\mu_k}} \binom{k_{ik}}{r_1 \ r_2 \ r_3 \ r_4} \times J(n_{\rho_{ik}}+1, n_{\rho_{jl}}+1, \alpha_{ik}, \alpha_{jl}; \mu_{ik}+1+2r_1+r_3+r_4; u) \quad (\text{A.13})$$

The final step is to evaluate the u -integration after inserting eqs.(A.13,A.5) into eq.(A.2). Considering

$$\begin{aligned} \langle ij|V_{II}|kl\rangle &= 32\pi^{\frac{3}{2}} \delta_{m_{kl},m_{ij}} g_{n_{zijkl}} \sum_{\mu_i=0}^{|m_i|} \binom{|m_i|}{\mu_i} \sum_{\mu_k=0}^{|m_k|} \binom{|m_k|}{\mu_k} \sum_{\substack{r_1+r_2+r_3+r_4=k_{ik} \\ r_3-r_4=-s_i\mu_i+s_k\mu_k}} \binom{k_{ik}}{r_1 \ r_2 \ r_3 \ r_4} \sum_{\zeta=0}^{\zeta \leq \frac{n_{zik}}{2}} \binom{n_{zik}}{2\zeta} \\ &\times \int_0^\infty du J(n_{\rho_{ik}}+1, n_{\rho_{jl}}+1, \alpha_{ik}, \alpha_{jl}; \mu_{ik}+1+2r_1+r_3+r_4; u) \cdot J(n_{zik}, n_{zjl}, \beta_{ik}, \beta_{jl}; 2\zeta; u) \end{aligned} \quad (\text{A.14})$$

shows that the solution of the electron-electron integral is now reduced to the integration

$$K(n_1, n_2, a_1, a_2; v; m_1, m_2, b_1, b_2; w) = \int_0^\infty du J(n_1, n_2, a_1, a_2; v; u) \cdot J(m_1, m_2, b_1, b_2; w; u) \quad (\text{A.15})$$

Up to a constant prefactor, the integrand in eq.(A.15) is of the type $g(u) = u^{2n_u} \cdot (1+au^2)^{r_a} (1+bu^2)^{r_b} (1+cu^2)^{r_c} (1+du^2)^{r_d}$ where $a = \frac{1}{a_1}$, $b = \frac{1}{b_1}$, $c = \frac{a_{12}}{a_1 a_2}$, $d = \frac{b_{12}}{b_1 b_2}$ are fixed real numbers given by the basis functions. The exponents depend on the summation indices which enter into the functions J , and $n_u := n_1+m_1-v-w$ is running over positive integer values. Further $r_a := \frac{n_2-n_1}{2}$ and $r_b := \frac{m_2-m_1}{2}$ are integers whereas $r_c := \frac{v-1-n_{12}}{2}$ is integer or half-integer and $r_d := \frac{w-1-m_{12}}{2}$ is always half-integer. The substitution $x := \frac{u^2}{1/d+u^2}$ with $du = \frac{1}{2}d^{-1/2}x^{-1/2}(1-x)^{-3/2} dx$ leads to

$$\int_0^\infty g(u) du = \frac{1}{2}d^{-n_u-\frac{1}{2}} \int_0^1 x^{n_u-\frac{1}{2}} (1-x)^{-r_{abcd}-n_u-\frac{3}{2}} (1+q_a x)^{r_a} (1+q_b x)^{r_b} (1+q_c x)^{r_c} dx \quad (\text{A.16})$$

where $r_{abcd} := r_a + r_b + r_c + r_d$ and $q_a := \frac{a}{d} - 1$, $q_b := \frac{b}{d} - 1$, $q_c := \frac{c}{d} - 1$. In order to reduce this integral to hypergeometric functions it is now necessary to multiply out one of the three last factors. This is possible since the basis functions can always be interchanged in such a way that one of the exponents r_a, r_b is

positive, say r_a . Then eq.(3.211) in ref.[23] can be used to obtain

$$\int_0^\infty g(u) du = \frac{1}{2} d^{-n_u - \frac{1}{2}} \sum_{s=0}^{r_a} \binom{r_a}{s} q_a^s \times B(-r_{abcd} - n_u - \frac{1}{2}, n_u + s + \frac{1}{2}) \times F_1(n_u + s + \frac{1}{2}, -r_b, -r_c, s - r_{abcd}; -q_b, -q_c) \quad (\text{A.17})$$

where B is the beta function and F_1 is the Appell hypergeometric function[24]. It is defined as double series, $F_1(a, b, b'; c; x, y) := \sum_{\nu=0}^\infty \frac{(a, \nu)(b, \nu)}{(c, \nu)(1, \nu)} {}_2F_1(a + \nu, b', c + \nu; y) x^\nu$ where ${}_2F_1(a, b, c; z) := \sum_{\mu=0}^\infty \frac{(a, \mu)(b, \mu)}{(c, \mu)(1, \mu)} z^\mu$ is the Gaussian hypergeometric function and $(a, \nu) := \frac{\Gamma(a+\nu)}{\Gamma(a)}$ is the Pochhammer symbol. Including all prefactors, we obtain for the integral K :

$$K(n_1, n_2, a_1, a_2, v; m_1, m_2, b_1, b_2, w) = \frac{1}{16} a_1^{-n_1 - \frac{1}{2}} a_2^{-\frac{n_{12}+1}{2}} \cdot \Gamma(\frac{v+1}{2}) \cdot \Gamma(\frac{n_{12}-v+1}{2}) \cdot (a_1 a_2)^{\frac{v}{2}} \times b_1^{-m_1 - \frac{1}{2}} b_2^{-\frac{m_{12}+1}{2}} \cdot \Gamma(\frac{w+1}{2}) \cdot \Gamma(\frac{m_{12}-w+1}{2}) \cdot (b_1 b_2)^{\frac{w}{2}} \times \int_0^\infty g(u) du \quad (\text{A.18})$$

where now the integral stands for the expression (A.17).

The final result is a *real* value for $\langle ij|V_{II}|kl\rangle$ obtained by inserting eq.(A.18) into eq.(A.14):

$$\begin{aligned} \langle ij|V_{II}|kl\rangle &= \pi^{\frac{3}{2}} \delta_{m_{kl}, m_{ij}} g_{n_{zijkl}} \cdot \alpha_{ik}^{-n_1 - \frac{1}{2}} \alpha_{jl}^{-\frac{n_{12}+1}{2}} \cdot \beta_{ik}^{-m_1 - \frac{1}{2}} \beta_{jl}^{-\frac{m_{12}+1}{2}} \sum_{\mu_i=0}^{|m_i|} \binom{|m_i|}{\mu_i} \sum_{\mu_k=0}^{|m_k|} \binom{|m_k|}{\mu_k} \\ &\times \sum_{\substack{r_1+r_2+r_3+r_4=k_{ik} \\ r_3-r_4=-s_i \mu_i + s_k \mu_k}} \binom{k_{ik}}{r_1 \ r_2 \ r_3 \ r_4} \Gamma(\frac{v+1}{2}) \cdot \Gamma(\frac{n_{12}-v+1}{2}) \cdot (\alpha_{ik} \alpha_{jl})^{\frac{v}{2}} \\ &\times \sum_{\substack{\zeta \leq \frac{n_{zijk}}{2} \\ \zeta=0 \\ w \text{ gerade}}} \binom{n_{zijk}}{2\zeta} \Gamma(\frac{1}{2} + \zeta) \cdot \Gamma(\frac{m_{12}+1}{2} - \zeta) \cdot (\beta_{ik} \beta_{jl})^\zeta \\ &\times d^{-n_u - \frac{1}{2}} \sum_{s=0}^{r_a} \binom{r_a}{s} q_a^s \cdot B(-r_{abcd} - n_u - \frac{1}{2}, n_u + s + \frac{1}{2}) \\ &\times F_1(n_u + s + \frac{1}{2}, -r_b, -r_c, s - r_{abcd}; -q_b, -q_c) \end{aligned} \quad (\text{A.19})$$

An overview over the various parameters entering into eq.(A.19) is given in appendix C where we briefly present the algorithm for the implementation of eq.(A.19). The direct implementation of eq.(A.19) yields already a factor of 5 to 10 with respect to the increase in speed compared with the common result derived in Cartesian coordinates in ref.[12]. However, by systematic exploitation of the symmetries the gain factor of CPU can further be raised to between 20 and 40.

B Symmetry properties of the electron-electron integral

In the present section we list the different types of symmetries for the expressions encountered in appendix A.

B.1 External symmetries

By an external symmetry we mean a permutation of basis functions which leave $\langle ij|V_{II}|kl\rangle$ invariant (up to complex conjugation). Such symmetries are firstly $\langle ij|V_{II}|kl\rangle = \langle ji|V_{II}|lk\rangle$ since the particles are indistinguishable, and secondly we have $\langle ij|V_{II}|kl\rangle = \langle kl|V_{II}|ij\rangle^*$ due to the hermiticity of V_{II} , in the case of our real matrix elements even $\langle ij|V_{II}|kl\rangle = \langle kl|V_{II}|ij\rangle$.

B.2 Internal symmetries

The integral $\langle ij|V_{II}|kl\rangle$ is also invariant under any manipulation of the basis functions which leave the integrals $I_z(u)$ and $I_{\rho\varphi}(u)$ in eq.(A.2) invariant separately. This class of internal transformations is larger than the class of permutations of basis functions since the parameters entering in $I_z(u)$ and $I_{\rho\varphi}(u)$ can be varied independently. $I_z(u)$ is invariant under the simultaneous exchanges $i \leftrightarrow j$ and $k \leftrightarrow l$ of indices only in the parameters β and n_z , and $I_{\rho\varphi}(u)$ stays unchanged under the analogous interchange of only the parameters α , n_ρ and m . Eq.(A.5) shows a further internal symmetry of $I_{\rho\varphi}(u)$: if the difference $m_i - m_k$ remains unchanged the parameters m_i and m_k can be varied arbitrarily as long as the constraint (3) can be fulfilled for some k_i and k_k , respectively (analogously for m_j and m_l). It is an interesting fact that the matrix element $\langle ij|V_{II}|kl\rangle$ in a subspace with $M = m_i + m_j = m_k + m_l$ possesses the same numerical value as some matrix elements involved in subspaces corresponding to some other value of M !

The internal symmetries can be exploited for achieving simultaneously $n_{\rho jl} \geq n_{\rho ik}$ and $n_{zjl} \geq n_{zik}$, i.e. in the function $g(u)$ (see eqs.(A.15,A.16)) *even both* parameters r_a and r_b can be assumed to be non-negative. A very important consequence of this is that due to the definition of F_1 (see paragraph below eq.(A.17)) its double series reduces to a sum over a *finite number* of expressions involving the Gaussian hypergeometric function ${}_2F_1(a, b; c; z)$ which is much simpler to evaluate than $F_1(a, b, b'; c; x, y)$.

B.3 Further symmetries

Assuming both parameters r_a and r_b to be non-negative, eq.(A.17) is also valid after interchanging $r_a \leftrightarrow r_b$ (and simultaneously $q_a \leftrightarrow q_b$), representing a new invariance transformation of $\langle ij|V_{II}|kl\rangle$.

C Implementation

In the following we present the algorithm for the implementation of eq.(A.19) for our calculations on helium.

1. Due the external symmetry $\langle ij|V_{II}|kl\rangle = \langle kl|V_{II}|ij\rangle$ it is sufficient to compute only the upper triangle of the matrix corresponding to V_{II} .
2. If $n_{\rho jl} - n_{\rho ik} < 0$, we use the external symmetry $\langle ij|V_{II}|kl\rangle = \langle ji|V_{II}|lk\rangle$ and interchange globally $i \leftrightarrow j$, $k \leftrightarrow l$, which achieves $r_a \geq 0$.

3. If then $n_{zjl} - n_{zik} < 0$, we use the internal symmetry of $I_z(u)$ and interchange $n_{zi} \leftrightarrow n_{zj}$, $n_{zk} \leftrightarrow n_{zl}$ as well as $\beta_i \leftrightarrow \beta_j$, $\beta_k \leftrightarrow \beta_l$, which achieves $r_b \geq 0$.
4. We introduce the following abbreviations for the fixed parameters independent on the summation indices of eq.(A.19):

name	definition	type	property
n_1	$= n_{\rho_{ik}} + 1$	integer	$1 \leq n_1$
n_{12}	$= n_{\rho_{ik}} + n_{\rho_{jl}} + 2$	even	$2 \leq n_{12}$
m_1	$= n_{zik}$	integer	$0 \leq m_1$
m_{12}	$= n_{zik} + n_{zjl}$	even	$0 \leq m_{12}$
r_a	$= \frac{n_{\rho_{jl}} - n_{\rho_{ik}}}{2}$	integer	$0 \leq r_a$
r_b	$= \frac{n_{zjl} - n_{zik}}{2}$	integer	$0 \leq r_b$
d	$= \frac{\beta_{ik} + \beta_{jl}}{\beta_{ik}\beta_{jl}}$	real	$1 < d$
$-q_a$	$= 1 - \frac{\beta_{ik}\beta_{jl}}{\alpha_{ik}(\beta_{ik} + \beta_{jl})}$	real	$-1 < q_a$
$-q_b$	$= \frac{\beta_{ik}}{\beta_{ik} + \beta_{jl}}$	real	$-1 < q_b < 0$
$-q_c$	$= 1 - \frac{(\alpha_{ik} + \alpha_{jl})\beta_{ik}\beta_{jl}}{(\beta_{ik} + \beta_{jl})\alpha_{ik}\alpha_{jl}}$	real	$-1 < q_c$

5. If then $r_a > r_b$, we interchange $r_a \leftrightarrow r_b$, $q_a \leftrightarrow q_b$, thereby minimizing the number of terms of the innermost summation in eq.(A.19).
6. Applying the internal symmetry transformation of suitably shifting the values of m_i and m_k , we replace both m_i and m_k by $m_i + 2s$ and $m_k + 2s$, respectively, where s is the highest possible integer such that $|m_i + 2s| \leq n_{\rho_i}$ and $|m_k + 2s| \leq n_{\rho_k}$. This step is very useful for decreasing the number of summations over the indices r_1, r_2, r_3, r_4 since raising m_i and m_k has the consequence that k_i and k_k must decrease for keeping n_{ρ_i} and n_{ρ_k} constant.
7. We apply the formula (A.19), and the parameters occuring therein depend on the summation indices according to the following definitions:

name	definition	type	property
v	$= \mu_{ik} + 1 + 2r_1 + r_3 + r_4$	integer	$1 \leq v \leq n_{\rho_{ik}} + 1$
w	$= 2\zeta$	even	$0 \leq w \leq n_{zik} - g_{n_{zik}}$
n_u	$= n_1 + m_1 - v - w$	integer	$g_{n_{zik}} \leq n_u \leq n_{\rho_{ik}} + n_{zik}$
r_c	$= \frac{v-1-n_{12}}{2}$	int. or half-int.	$-\frac{n_{\rho_{ik}} + n_{\rho_{jl}}}{2} - 1 \leq r_c \leq -\frac{n_{\rho_{jl}}}{2} - 1$
r_d	$= \frac{w-1-m_{12}}{2}$	half-integer	$-\frac{1+n_{zik}+n_{zjl}}{2} \leq r_d \leq -\frac{1+g_{n_{zik}}+n_{zjl}}{2} < 0$
r_{abcd}	$= -n_1 - m_1 + \frac{v+w}{2} - 1$	int. or half-int.	$-n_{\rho_{ik}} - n_{zik} - \frac{3}{2} \leq r_{abcd} \leq \frac{-n_{\rho_{ik}} - n_{zik} - 3 - g_{n_{zik}}}{2} < 0$

8. Although in principle $F_1(a, b, b'; c; x, y)$ is a double power series in the arguments x, y with convergence radii $|x| < 1$ and $|y| < 1$ and although in our case even both arguments may happen to lie close to 1, we do not have to care about the power series in x . The reason is that the corresponding series terminates after r_b terms because the negative integer $-r_b$ enters as second parameter argument into F_1 in eq.(A.19). The sum terms in F_1 each involve once the Gaussian hypergeometric function, and since their arguments are related, it is possible to use a continued fraction representation for the ratio $\frac{{}_2F_1(a+1, b, c+1, z)}{{}_2F_1(a, b, c, z)}$ in order to establish a recursion law which is stable over the typically $r_b < 10$ recursions. Therefore, for each occurrence of F_1 , it was only necessary to evaluate a single time the Gaussian hypergeometric function ${}_2F_1$, which is not always simple but very efficiently possible by means of *fast analytical continuation formulas*. Several of them are given in eqs.(15.3.3-12) in ref.[25], a much larger set of such continuation formulas is presented in ref.[26].

We point out that without such a systematic analysis of the electron-electron integral as well as the Appell hypergeometric function F_1 and in particular the Gaussian hypergeometric function ${}_2F_1$, the computation of many excited helium states for nonzero magnetic quantum number for many different field strengths would not have been possible.

References

- [1] H. Friedrich, Phys.Rev. **A 26**, 1827 (1982)
- [2] W. Rösner, G. Wunner, H. Herold and H. Ruder, J.Phys. **B 17**, 29 (1984)
- [3] D. Wintgen and H. Friedrich, J.Phys. **B 19**, 991 (1986)
- [4] M.V. Ivanov, J.Phys. **B 21**, 447 (1988)
- [5] Yu.P. Kravchenko, M.A. Liberman and B. Johansson, Phys.Rev. **A 54**, 287 (1996)
- [6] H. Ruder, G. Wunner, H. Herold und F. Geyer, Atoms in Strong Magnetic Fields, Springer Verlag A-A 1994.
- [7] P. Schmelcher and W. Schweizer (Eds.), Atoms and Molecules in Strong External Fields, Plenum Press 1998
- [8] R.F. Green and J. Liebert, Pub. Astr. Soc. Pac 93, 105 (1980)
- [9] G.D. Schmidt, W.B. Latter, C.B. Foltz, Astrophysical Journal 350, 758 (1990)
- [10] G.D. Schmidt, R.G. Allen, P.S. Smith, J. Liebert, Astrophysical Journal 463, 320 (1996)
- [11] S. Jordan, P. Schmelcher, W. Becken and W. Schweizer, Astronomy & Astrophysics Letters **336**, L33-L36 (1998)
- [12] W. Becken, P. Schmelcher and F.K. Diakonos, J. Phys.**B 32**, 1557 (1999)
- [13] M.D. Jones and G. Ortiz, Phys.Rev. **A 59**, 2875 (1999)
- [14] A. Scrinzi, Phys.Rev. **A 58**, 3879 (1998)
- [15] V.B. Pavlov-Verevkin and B.I. Zhilinskii, Phys. Letters, **78A**, no. 3, 244 (1980)
- [16] G.W.F. Drake and Z.-C. Yan, Phys.Rev. **A 46** 2378 (1992)
- [17] D.M. Larsen, Phys.Rev. **B 20**, 20 (1979)
- [18] M.D. Jones, G. Ortiz, D.M. Ceperley, Phys.Rev. **A 54**, 219 (1996)
- [19] M.D. Jones, G. Ortiz, D.M. Ceperley, Phys.Rev. **E 55**, 6202 (1997)
- [20] M.V. Ivanov, J.Phys. **B 27**, 4513 (1994)
- [21] G. Thurner, H. Körbel, M. Braun, H. Herold, H. Ruder and G. Wunner, J.Phys. **B 26**, 4719 (1993)

- [22] K. Singer, Proc. R. Soc. Lond. **A 402**, 412 (1960)
- [23] I. S. Gradshteyn and I. M. Ryzhik, Table of integrals, series, and products, Academic Press, 1980
- [24] P. Appell et J. Kampé de Fériet, Les fonctions hypergéométriques et hypersphériques, Gauthier-Villars et Cie, Editeurs, Paris 1926
- [25] M. Abramowitz and I.A. Stegun, Handbook of mathematical functions, Dover Publications, 1972
- [26] W. Becken and P. Schmelcher, *submitted to Journal of Computational and Applied Mathematics*

Captions

Fig.1. Ionization energies of the singlet and triplet states $k^1(-1)^+$ and $n^3(-1)^+$, $k = 1, \dots, 5$, $n = 1, \dots, 5$. The solid lines correspond to the singlet states, the dashed ones show the triplet states.

Fig.2. Ionization energies of the singlet and triplet states $k^1(-1)^-$ and $n^3(-1)^-$, $k = 1, \dots, 5$, $n = 1, \dots, 5$. The solid lines correspond to the singlet states, the dashed ones show the triplet states.

Fig.1

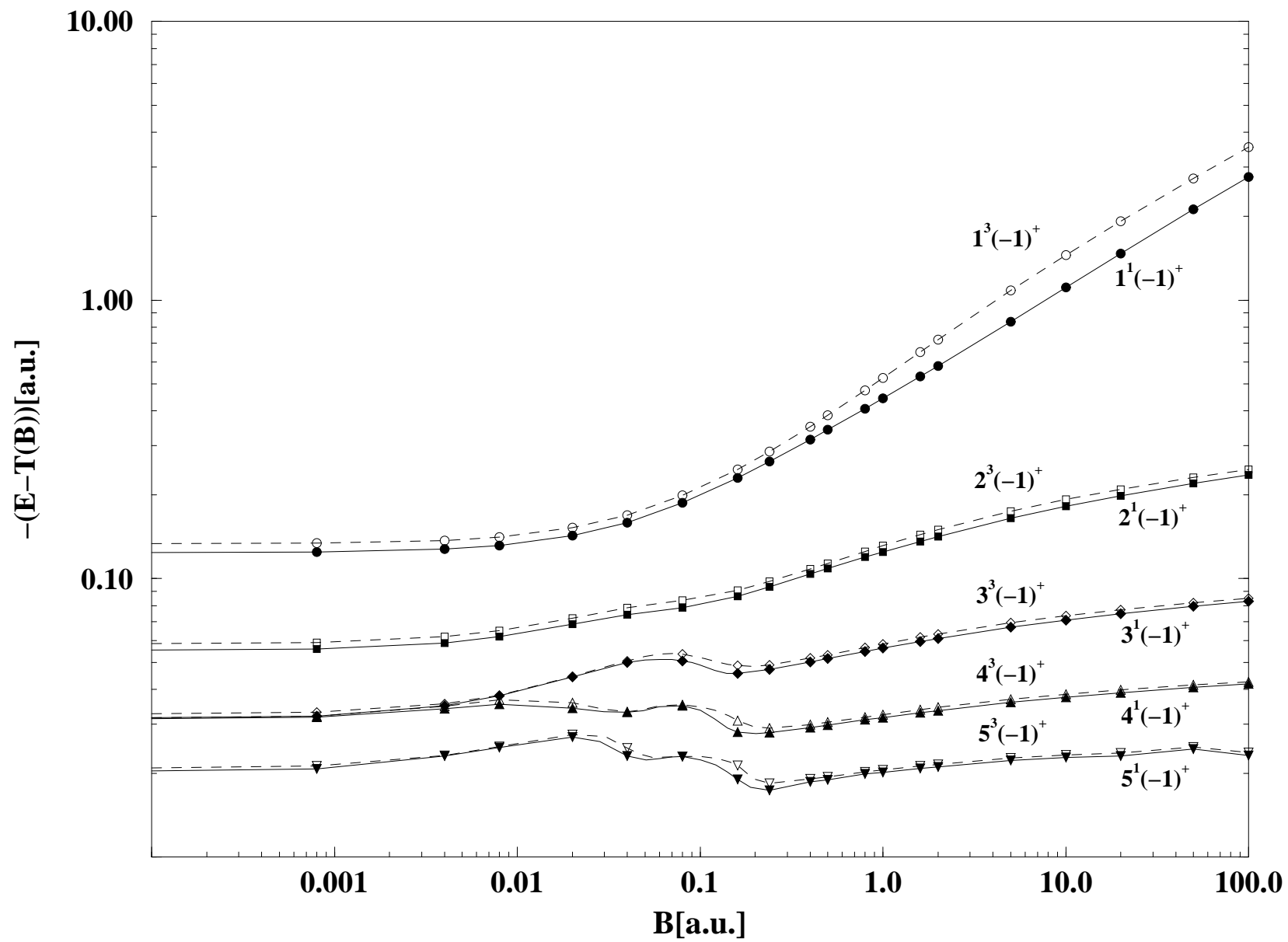
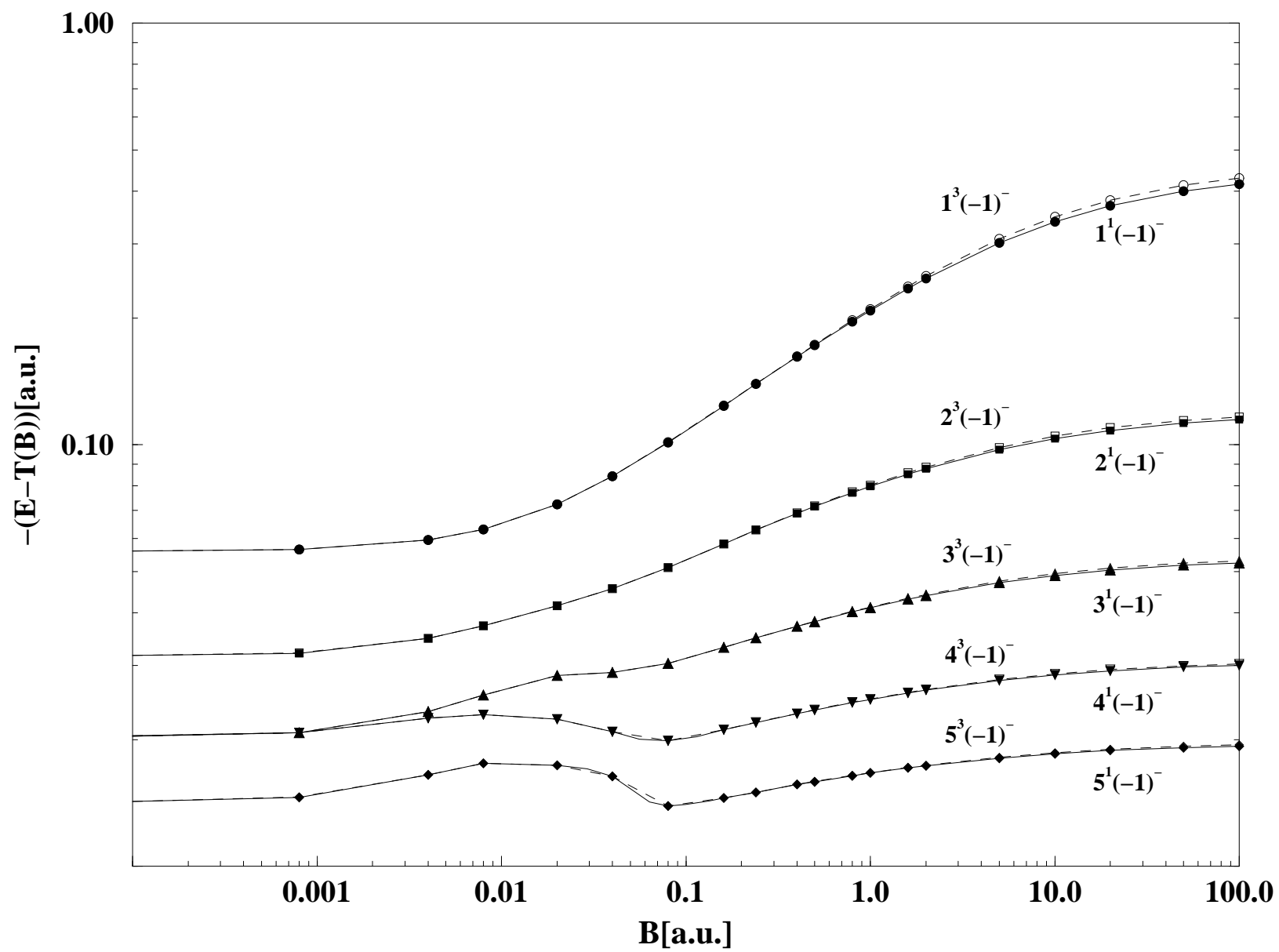


Fig.2



Tables

Table 1: Total energies E of the singlet state $1^1(-1)^+$, one-electron ionization threshold T and, if available, best energy values given in the literature, as a function of the magnetic field strength B

B	$E(1^1(-1)^+)$	literature	T
0.0000	-2.123774	-2.12384343087 ^a	-2.000
0.0008	-2.124179		-1.999599960
0.004	-2.125732		-1.997999000
0.008	-2.127580		-1.995995995
0.020	-2.132539		-1.989975001
0.040	-2.139008		-1.979900008
0.080	-2.146622		-1.959600176
0.160	-2.148448		-1.918402804
0.240	-2.139976		-1.876414090
0.400	-2.105987		-1.790105922
0.500	-2.077302	-2.0750 ^b	-1.734628064
0.800	-1.969560		-1.561526260
1.000	-1.884875	-1.8800 ^b	-1.440989741
1.600	-1.590118		-1.058421519
2.000	-1.368986	-1.3591 ^b	-0.788842154
5.000	0.619265		1.456132354
10.000	4.500982		5.609851957
20.000	13.010551		14.47840453
50.000	40.339488		42.45369755
100.000	87.671288		90.43945348

^a Drake et al. (1992) [16]

^b Larsen (1979) [17]

Table 2: Total energies E of the excited singlet states $\nu^1(-1)^+$ for $2 \leq \nu \leq 5$ as a function of the magnetic field strength B as well as field free reference values

B	$E(2^1(-1)^+)$	$E(3^1(-1)^+)$	$E(4^1(-1)^+)$	$E(5^1(-1)^+)$
0.0000	-2.055124	-2.031253	-2.031060	-2.020002
0.0000 (lit.)	-2.055146362 ^a	-2.031255144 ^a	-2.03106965 ^a	-2.020002937 ^a
0.0008	-2.055514	-2.031638	-2.031422	-2.020356
0.004	-2.056834	-2.032905	-2.032089	-2.021046
0.008	-2.057978	-2.033939	-2.031432	-2.020791
0.020	-2.058622	-2.034384	-2.024218	-2.017013
0.040	-2.053994	-2.029964	-2.013028	-2.003001
0.080	-2.038112	-2.010281	-1.994622	-1.982587
0.160	-2.004984	-1.964022	-1.946526	-1.937449
0.240	-1.970004	-1.923549	-1.904394	-1.893803
0.400	-1.893976	-1.840324	-1.819308	-1.808757
0.500	-1.843343	-1.786317	-1.764444	-1.753581
0.800	-1.680951	-1.616388	-1.592658	-1.581405
1.000	-1.565692	-1.497369	-1.472743	-1.461154
1.600	-1.194554	-1.117980	-1.091462	-1.079247
2.000	-0.930508	-0.849891	-0.822478	-0.809928
5.000	1.291512	1.389207	1.420194	1.433857
10.000	5.428064	5.538802	5.572339	5.586918
20.000	14.279839	14.403512	14.439480	14.455341
50.000	42.233602	42.374094	42.413014	42.429203
100.000	90.203618	90.356573	90.397606	90.416255

^a Drake et al. (1992) [16]

Table 3: Total energies E of the triplet states $\nu_{-1}^3(-1)^+$ ($S_z = -1$) for $1 \leq \nu \leq 5$ as a function of the magnetic field strength B . We have also provided the results given in the literature so far.

	$E(1^3(-1)^+)$		$E(2^3(-1)^+)$		$E(3^3(-1)^+)$		$E(4^3(-1)^+)$	$E(5^3(-1)^+)$
B	this work	literature	this work	literature	this work	literature	this work	this work
0.0000	-2.133149	-2.133164191 ^a	-2.058076	-2.058081084 ^a	-2.032322	-2.032324354 ^a	-2.031253	-2.020550
0.0008	-2.134349	-2.1326 ^c	-2.059266	-2.0588 ^c	-2.033487		-2.031255168 ^a	-2.020551187 ^a
0.004	-2.139109	-2.1374 ^c	-2.063816	-2.0633 ^c	-2.037489		-2.032438	-2.021661
0.008	-2.144983	-2.1437(7) ^d	-2.069049	-2.0689(4) ^d	-2.042110	-2.0407(3) ^d	-2.036839	-2.025180
0.020	-2.162112		-2.082183		-2.054609		-2.040765	-2.028940
0.040	-2.189128	-2.187300 ^f	-2.098532	-2.096752 ^f	-2.070637		-2.045891	-2.037572
0.080	-2.238504	-2.2384(3) ^g	-2.123337	-2.1231(5) ^g	-2.093337	-2.0898(3) ^g	-2.053178	-2.044517
0.160	-2.325189		-2.169263		-2.127206		-2.074828	-2.062590
0.240	-2.402393		-2.214084	-2.210304 ^f	-2.165492		-2.109343	-2.099747
0.400	-2.540763	-2.5366 ^c	-2.298465	-2.2972 ^h	-2.241932	-2.2413 ^h	-2.145502	-2.134821
0.500	-2.620021	-2.6185 ^b	-2.348197		-2.287934		-2.220053	-2.209244
0.800	-2.835619	-2.8356(2) ^g	-2.486853	-2.4869(11) ^g	-2.418154	-2.4189(2) ^g	-2.265163	-2.254042
1.000	-2.965504	-2.9638 ^b	-2.572178		-2.499237		-2.393403	-2.381809
1.600	-3.308774	-3.3079(7) ^d	-2.802301	-2.8015(8) ^d	-2.720071	-2.6950(12) ^d	-2.473517	-2.461576
2.000	-3.508911	-3.5063 ^b	-2.938822		-2.720071		-2.692304	-2.679694
5.000	-4.625491	-4.6173 ^e	-3.718569		-2.852078		-2.823349	-2.810394
10.000	-5.839475	-5.8295 ^e	-4.582689		-3.613233		-3.580744	-3.566622
20.000	-7.440556	-7.4277 ^e	-5.731115		-4.463680		-4.428595	-4.413579
50.000	-10.28410	-10.2644 ^e	-7.777100		-5.598915		-4.428595	-5.545260
100.00	-13.10478	-13.0764 ^e	-9.806638		-7.628163		-5.561423	-7.571207
					-9.645518		-7.587802	-9.584339
							-9.603141	

^a Drake et al. (1992) [16]

^b Larsen (1979) [17]

^c Jones et al. (1996) [18]

^d Jones et al. (1997) [19]

^e Ivanov (1994) [20]

^f Thurner et al. (1993) [21]

^g Jones et al. (1999) [13]

^h ETG Hartree-Fock energies (Jones et al. (1999) [13])

Table 4: Total energies E of the states $\nu^1(-1)^-$, $1 \leq \nu \leq 5$ as a function of the magnetic field strength B as well as field free reference values. Reference values for finite field strength are not available in the literature so far.

B	$E(1^1(-1)^-)$	$E(2^1(-1)^-)$	$E(3^1(-1)^-)$	$E(4^1(-1)^-)$	$E(5^1(-1)^-)$
0.0000	-2.055613 -2.055620733 ^a	-2.031277 -2.031279846 ^a	-2.020014 -2.020015836 ^a	-2.020000 -2.020000711 ^a	-2.013892 -2.013898227 ^a
0.0008	-2.056007	-2.031653	-2.020375	-2.020344	-2.014196
0.004	-2.057469	-2.032717	-2.021323	-2.020478	-2.014483
0.008	-2.059049	-2.033191	-2.021527	-2.018934	-2.013542
0.020	-2.062299	-2.031471	-2.018372	-2.012348	-2.007346
0.040	-2.064207	-2.025446	-2.008719	-2.000788	-1.996278
0.080	-2.060968	-2.010768	-1.989904	-1.979451	-1.973516
0.160	-2.042173	-1.976616	-1.951446	-1.939499	-1.932936
0.240	-2.015792	-1.939171	-1.911235	-1.898364	-1.891395
0.400	-1.951742	-1.858850	-1.827207	-1.813144	-1.805743
0.500	-1.906870	-1.806041	-1.772722	-1.758134	-1.750501
0.800	-1.757739	-1.638598	-1.601676	-1.585991	-1.577931
1.000	-1.649285	-1.520740	-1.482091	-1.465894	-1.457643
1.600	-1.293330	-1.143718	-1.101454	-1.084209	-1.075561
2.000	-1.036760	-0.876696	-0.832747	-0.815025	-0.806167
5.000	1.154910	1.358659	1.409032	1.428522	1.438083
10.000	5.271756	5.506378	5.560823	5.581393	5.591327
20.000	14.109153	14.370201	14.427890	14.449299	14.459536
50.000	42.053685	42.341109	42.401827	42.424005	42.434562
100.000	90.023511	90.324738	90.386944	90.409492	90.420161

^a Drake et al. (1992) [16]

Table 5: Total energies E of the triplet states $\nu_{-1}^3(-1)^-$ ($S_z = -1$) for $1 \leq \nu \leq 5$ as a function of the magnetic field strength B . We have also provided the results given in the literature so far.

	$E(1^3(-1)^-)$		$E(2^3(-1)^-)$		$E(3^3(-1)^-)$		$E(4^3(-1)^-)$	$E(5^3(-1)^-)$
B	this work	literature	this work	literature	this work	literature	this work	this work
0.0000	-2.055629	-2.055636309 ^a	-2.031286	-2.031288847 ^a	-2.020020	-2.020021027 ^a	-2.020000 -2.020000711 ^a	-2.013895 -2.013901415 ^a
0.0008	-2.056824	-2.056766 ^f	-2.032463	-2.032436 ^f	-2.021176		-2.021148	-2.014998
0.004	-2.061486	-2.061428 ^f	-2.036727	-2.036694 ^f	-2.025324		-2.024483	-2.018484
0.008	-2.067062	-2.067000 ^f	-2.041202	-2.0413(9) ^d	-2.029529	-2.0266(7) ^d	-2.026940	-2.021545
0.020	-2.082319		-2.051485		-2.038378		-2.032348	-2.027352
0.040	-2.104234	-2.103728 ^f	-2.065465	-2.057738 ^f	-2.048734		-2.040795	-2.036278
0.080	-2.141017	-2.1414(3) ^g	-2.090793	-2.0912(2) ^g	-2.069919	-2.0696(4) ^g	-2.059460	-2.053523
0.160	-2.202291	-2.193460 ^f	-2.136663		-2.111468		-2.099511	-2.092944
0.240	-2.256006	-2.238396 ^f	-2.179246		-2.151267		-2.138381	-2.131405
0.400	-2.352208	-2.3512 ^h	-2.258990	-2.2588 ^h	-2.227265	-2.2271 ^h	-2.213172	-2.205759
0.500	-2.407521		-2.306225		-2.272795		-2.258169	-2.250521
0.800	-2.559005	-2.5577(4) ^g	-2.438913	-2.4392(5) ^g	-2.401794	-2.4022(4) ^g	-2.386047	-2.377963
1.000	-2.650973		-2.521134		-2.482236		-2.465962	-2.457680
1.600	-2.896192	-2.8964(7) ^d	-2.744310	-2.7394(8) ^d	-2.701661	-2.6436(17) ^d	-2.684304	-2.675612
2.000	-3.040304		-2.877390		-2.832986		-2.815133	-2.806227
5.000	-3.851883		-3.642446		-3.591326		-3.571636	-3.562005
10.000	-4.737490		-4.494996		-4.439609		-4.418795	-4.408774
20.000	-5.902110		-5.631390		-5.572603		-5.550913	-5.540577
50.000	-7.959094		-7.660647		-7.598710		-7.576226	-7.565565
100.00	-9.989376		-9.677020		-9.613592		-9.590738	-9.579962

^a Drake et al. (1992) [16]

^d Jones et al. (1997) [19]

^f Thurner et al. (1993) [21]

^g Jones et al. (1999) [13]

^h ETG Hartree-Fock energies (Jones et al. (1999) [13])

Table 6: Overview over all of the stationary points found in the singlet $\Delta M = 0$ transitions $\mu^1(-1)^+ \rightarrow \nu^1(-1)^-$ for $\mu = 1, \dots, 5$, $\nu = 1, \dots, 5$ in the range $0 \leq B \leq 100a.u.$. The main part of the errors arises due to the interpolation over the relatively crude grid of field strengths. For high wavelengths, the finite accuracy of the energy values themselves contributes also to error in the energies.

Component $\nu^{2S+1}M^{(-1)^{\Pi_z}}$	wavelength/ \AA	position $B/a.u.$	max/min
$2^1(-1)^- \rightarrow 2^1(-1)^+$	15915 ± 50	0.035 ± 0.003	min
$2^1(-1)^- \rightarrow 2^1(-1)^+$	16770 ± 85	0.098 ± 0.007	max
$2^1(-1)^- \rightarrow 3^1(-1)^+$	13649.7 ± 3.0	26.06 ± 0.04	min
$3^1(-1)^- \rightarrow 3^1(-1)^+$	20505 ± 80	0.0542 ± 0.0004	min
$3^1(-1)^- \rightarrow 3^1(-1)^+$	37139 ± 20	0.213 ± 0.001	max
$3^1(-1)^- \rightarrow 4^1(-1)^+$	39258 ± 50	16.5 ± 0.3	min
$4^1(-1)^- \rightarrow 4^1(-1)^+$	29340 ± 550	0.08 ± 0.01	min
$4^1(-1)^- \rightarrow 4^1(-1)^+$	76600 ± 600	0.29 ± 0.01	max
$5^1(-1)^- \rightarrow 4^1(-1)^+$	25417.4 ± 30	0.00675 ± 0.00004	min
$5^1(-1)^- \rightarrow 4^1(-1)^+$	27502 ± 30	0.03076 ± 0.00001	max
$5^1(-1)^- \rightarrow 4^1(-1)^+$	18500 ± 1200	0.059 ± 0.002	min
$5^1(-1)^- \rightarrow 4^1(-1)^+$	35220 ± 300	0.23 ± 0.01	max
$5^1(-1)^- \rightarrow 5^1(-1)^+$	72600 ± 5200	0.046 ± 0.006	max
$5^1(-1)^- \rightarrow 5^1(-1)^+$	45100 ± 4000	0.095 ± 0.006	min
$5^1(-1)^- \rightarrow 5^1(-1)^+$	208000 ± 12000	0.290 ± 0.015	max

Table 7: Same as Table 6 but for the triplet $\Delta M = 0$ transitions
 $\mu^3(-1)^+ \rightarrow \nu^3(-1)^-$ for $\mu = 1, \dots, 5$, $\nu = 1, \dots, 5$

Component $\nu^{2S+1}M^{(-1)^{\Pi_z}}$	wavelength/ \AA	position $B/a.u.$	max/min
$2^3(-1)^- \rightarrow 3^3(-1)^+$	603000 ± 11000	0.00320 ± 0.00001	max
$2^3(-1)^- \rightarrow 3^3(-1)^+$	85000 ± 3200	0.036 ± 0.002	min
$2^3(-1)^- \rightarrow 3^3(-1)^+$	139400 ± 700	31 ± 5	min
$3^3(-1)^- \rightarrow 3^3(-1)^+$	37550 ± 160	0.0034 ± 0.0009	max
$3^3(-1)^- \rightarrow 3^3(-1)^+$	17700 ± 300	0.059 ± 0.001	min
$3^3(-1)^- \rightarrow 3^3(-1)^+$	32200 ± 60	0.270 ± 0.006	max
$3^3(-1)^- \rightarrow 4^3(-1)^+$	39240 ± 200	0.0045 ± 0.0015	min
$3^3(-1)^- \rightarrow 4^3(-1)^+$	40751 ± 10	20.0 ± 0.5	min
$4^3(-1)^- \rightarrow 3^3(-1)^+$	12930 ± 240	0.063 ± 0.003	min
$4^3(-1)^- \rightarrow 3^3(-1)^+$	16864 ± 33	0.215 ± 0.004	max
$4^3(-1)^- \rightarrow 4^3(-1)^+$	32340 ± 270	0.012 ± 0.0006	min
$4^3(-1)^- \rightarrow 4^3(-1)^+$	38800 ± 1600	0.03 ± 0.002	max
$4^3(-1)^- \rightarrow 4^3(-1)^+$	29460 ± 200	0.081 ± 0.008	min
$4^3(-1)^- \rightarrow 4^3(-1)^+$	66600 ± 200	0.34 ± 0.01	max
$4^3(-1)^- \rightarrow 5^3(-1)^+$	87175 ± 60	0.0196 ± 0.0002	min
$5^3(-1)^- \rightarrow 3^3(-1)^+$	11170 ± 180	0.065 ± 0.004	min
$5^3(-1)^- \rightarrow 3^3(-1)^+$	13470 ± 30	0.2002 ± 0.0009	max
$5^3(-1)^- \rightarrow 4^3(-1)^+$	23630 ± 40	0.0098 ± 0.0005	min
$5^3(-1)^- \rightarrow 4^3(-1)^+$	28200 ± 1000	0.031 ± 0.003	max
$5^3(-1)^- \rightarrow 4^3(-1)^+$	21050 ± 520	0.088 ± 0.01	min
$5^3(-1)^- \rightarrow 4^3(-1)^+$	32680 ± 340	0.23 ± 0.03	max
$5^3(-1)^- \rightarrow 5^3(-1)^+$	42200 ± 1700	0.015 ± 0.001	min
$5^3(-1)^- \rightarrow 5^3(-1)^+$	55790 ± 320	0.046 ± 0.002	max
$5^3(-1)^- \rightarrow 5^3(-1)^+$	48400 ± 960	0.100 ± 0.004	min
$5^3(-1)^- \rightarrow 5^3(-1)^+$	144000 ± 8000	0.30 ± 0.01	max
$5^3(-1)^- \rightarrow 5^3(-1)^+$	80200 ± 500	49.4 ± 7	min

Table 8: Overview over all of the stationary points found in the singlet $|\Delta M| = 1$ transitions within the subspace of positive z -parity, $\mu^1(-1)^+ \rightarrow \nu^1 0^+$ for $\mu = 1, \dots, 5$, $\nu = 1, \dots, 5$ in the range $0 \leq B \leq 100 a.u.$.

Component $\nu^{2S+1}M^{(-1)^{\Pi_z}}$	wavelength/ \AA	position $B/a.u.$	max/min
$1^1 0^+ \rightarrow 1^1(-1)^+$	608.1 ± 0.3	0.1672 ± 0.0015	max
$1^1 0^+ \rightarrow 2^1(-1)^+$	539.95 ± 0.25	0.0160 ± 0.0007	max
$1^1 0^+ \rightarrow 3^1(-1)^+$	524.83 ± 0.24	0.017 ± 0.002	max
$1^1 0^+ \rightarrow 4^1(-1)^+$	523.37 ± 0.22	0.004 ± 0.001	max
$1^1 0^+ \rightarrow 5^1(-1)^+$	516.80 ± 0.22	0.0046 ± 0.0008	max
$2^1 0^+ \rightarrow 2^1(-1)^+$	5285 ± 3	0.021 ± 0.003	max
$2^1 0^+ \rightarrow 2^1(-1)^+$	4812 ± 30	0.11 ± 0.01	min
$2^1 0^+ \rightarrow 3^1(-1)^+$	4125 ± 3	0.021 ± 0.003	max
$2^1 0^+ \rightarrow 3^1(-1)^+$	3417 ± 10	0.183 ± 0.005	min
$2^1 0^+ \rightarrow 3^1(-1)^+$	3795.8 ± 0.5	0.802 ± 0.008	max
$2^1 0^+ \rightarrow 4^1(-1)^+$	4006.2 ± 0.8	0.004 ± 0.001	max
$2^1 0^+ \rightarrow 4^1(-1)^+$	3015 ± 10	0.20 ± 0.01	min
$2^1 0^+ \rightarrow 4^1(-1)^+$	3177.7 ± 1.0	0.661 ± 0.005	max
$2^1 0^+ \rightarrow 5^1(-1)^+$	3651.7 ± 1.4	0.0050 ± 0.0005	max
$2^1 0^+ \rightarrow 5^1(-1)^+$	2825 ± 3	0.22 ± 0.01	min
$2^1 0^+ \rightarrow 5^1(-1)^+$	2950.4 ± 1.7	0.637 ± 0.006	max
$3^1 0^+ \rightarrow 3^1(-1)^+$	22030 ± 65	0.034 ± 0.001	max
$3^1 0^+ \rightarrow 3^1(-1)^+$	12634.5 ± 5.4	0.177 ± 0.002	min
$3^1 0^+ \rightarrow 4^1(-1)^+$	15809 ± 40	0.00576 ± 0.00008	max
$3^1 0^+ \rightarrow 4^1(-1)^+$	8270 ± 150	0.195 ± 0.005	min
$3^1 0^+ \rightarrow 4^1(-1)^+$	11765 ± 6	1.43 ± 0.02	max
$3^1 0^+ \rightarrow 5^1(-1)^+$	11533 ± 26	0.011 ± 0.002	max
$3^1 0^+ \rightarrow 5^1(-1)^+$	7170 ± 20	0.210 ± 0.005	min
$3^1 0^+ \rightarrow 5^1(-1)^+$	9004.4 ± 5.5	1.08 ± 0.02	max
$4^1 0^+ \rightarrow 4^1(-1)^+$	19840 ± 290	0.004 ± 0.002	max
$4^1 0^+ \rightarrow 4^1(-1)^+$	16190 ± 170	0.024 ± 0.003	min
$4^1 0^+ \rightarrow 4^1(-1)^+$	48900 ± 1400	0.074 ± 0.009	max
$4^1 0^+ \rightarrow 4^1(-1)^+$	26100 ± 1700	0.194 ± 0.004	min
$4^1 0^+ \rightarrow 5^1(-1)^+$	13283 ± 8	0.0065 ± 0.0004	max
$4^1 0^+ \rightarrow 5^1(-1)^+$	10490 ± 550	0.0285 ± 0.0005	min
$4^1 0^+ \rightarrow 5^1(-1)^+$	21520 ± 220	0.092 ± 0.003	max
$4^1 0^+ \rightarrow 5^1(-1)^+$	17100 ± 230	0.210 ± 0.003	max

Table 9: Same as Table 8 but for the triplet $|\Delta M| = 1$ transitions within the subspace of positive z -parity, $\mu^3(-1)^+ \rightarrow \nu^3 0^+$ for $\mu = 1, \dots, 5$, $\nu = 1, \dots, 5$.

Component $\nu^{2S+1}M^{(-1)^{\Pi_z}}$	wavelength/ \AA	position $B/a.u.$	max/min
$1^3 0^+ \rightarrow 2^3(-1)^+$	4058.6 ± 0.4	0.0214 ± 0.0001	max
$1^3 0^+ \rightarrow 2^3(-1)^+$	3580 ± 2	0.178 ± 0.002	min
$1^3 0^+ \rightarrow 3^3(-1)^+$	3258.1 ± 0.25	0.020 ± 0.001	max
$1^3 0^+ \rightarrow 3^3(-1)^+$	2615 ± 5	0.25 ± 0.02	min
$1^3 0^+ \rightarrow 3^3(-1)^+$	3090.1 ± 0.3	1.757 ± 0.004	max
$1^3 0^+ \rightarrow 4^3(-1)^+$	3210 ± 2	0.00576 ± 0.00008	max
$1^3 0^+ \rightarrow 4^3(-1)^+$	2336 ± 5	0.28 ± 0.01	min
$1^3 0^+ \rightarrow 4^3(-1)^+$	2600.4 ± 0.5	1.460 ± 0.009	max
$1^3 0^+ \rightarrow 5^3(-1)^+$	2959.2 ± 0.7	0.0047 ± 0.001	max
$1^3 0^+ \rightarrow 5^3(-1)^+$	2208 ± 3	0.299 ± 0.005	min
$1^3 0^+ \rightarrow 5^3(-1)^+$	2428.1 ± 0.5	1.379 ± 0.009	max
$2^3 0^+ \rightarrow 3^3(-1)^+$	17690 ± 80	0.047 ± 0.002	max
$2^3 0^+ \rightarrow 3^3(-1)^+$	11058.2 ± 2.0	0.238 ± 0.005	min
$2^3 0^+ \rightarrow 4^3(-1)^+$	12990 ± 32	0.0065 ± 0.0004	max
$2^3 0^+ \rightarrow 4^3(-1)^+$	7410 ± 40	0.27 ± 0.02	min
$2^3 0^+ \rightarrow 4^3(-1)^+$	10485 ± 9	2.93 ± 0.07	max
$2^3 0^+ \rightarrow 5^3(-1)^+$	9711 ± 13	0.013 ± 0.003	max
$2^3 0^+ \rightarrow 5^3(-1)^+$	6250 ± 40	0.29 ± 0.01	min
$2^3 0^+ \rightarrow 5^3(-1)^+$	8031.8 ± 1.7	2.14 ± 0.08	max
$3^3 0^+ \rightarrow 4^3(-1)^+$	20450 ± 120	0.007 ± 0.001	max
$3^3 0^+ \rightarrow 4^3(-1)^+$	14850 ± 300	0.035 ± 0.003	min
$3^3 0^+ \rightarrow 4^3(-1)^+$	37220 ± 680	0.094 ± 0.003	max
$3^3 0^+ \rightarrow 4^3(-1)^+$	26080 ± 250	0.281 ± 0.009	min
$3^3 0^+ \rightarrow 5^3(-1)^+$	13320 ± 3	0.0078 ± 0.0009	max
$3^3 0^+ \rightarrow 5^3(-1)^+$	11150 ± 560	0.032 ± 0.003	min
$3^3 0^+ \rightarrow 5^3(-1)^+$	20300 ± 1000	0.114 ± 0.007	max
$3^3 0^+ \rightarrow 5^3(-1)^+$	16030 ± 210	0.29 ± 0.01	min
$3^3 0^+ \rightarrow 5^3(-1)^+$	24864 ± 11	4.19 ± 0.08	max
$4^3 0^+ \rightarrow 4^3(-1)^+$	296800 ± 8500	0.009 ± 0.001	max
$4^3 0^+ \rightarrow 4^3(-1)^+$	297000 ± 8500	0.26 ± 0.02	max
$4^3 0^+ \rightarrow 5^3(-1)^+$	42500 ± 1300	0.017 ± 0.002	max
$4^3 0^+ \rightarrow 5^3(-1)^+$	82600 ± 3300	0.15 ± 0.02	max
$4^3 0^+ \rightarrow 5^3(-1)^+$	46400 ± 2000	0.29 ± 0.02	min
$4^3 0^+ \rightarrow 5^3(-1)^+$	240400 ± 1400	8.3 ± 0.5	max

Table 10: Overview over all of the stationary points found in the singlet $|\Delta M| = 1$ transitions within the subspace of negative z -parity, $\mu^1(-1)^- \rightarrow \nu^1 0^-$ for $\mu = 1, \dots, 5$, $\nu = 1, \dots, 5$.

Component $\nu^{2S+1}M^{(-1)\Pi_z}$	wavelength/ \AA	position $B/a.u.$	max/min
$2^1(-1)^- \rightarrow 1^1 0^-$	5056 ± 22	0.0088 ± 0.0002	max
$3^1(-1)^- \rightarrow 1^1 0^-$	4477 ± 18	0.0070 ± 0.0003	max
$3^1(-1)^- \rightarrow 2^1 0^-$	13875 ± 42	0.0105 ± 0.0001	max
$3^1(-1)^- \rightarrow 3^1 0^-$	56300 ± 1500	0.0139 ± 0.0015	max
$3^1(-1)^- \rightarrow 3^1 0^-$	50841 ± 100	0.0387 ± 0.0035	min
$4^1(-1)^- \rightarrow 1^1 0^-$	4442 ± 20	0.0022 ± 0.0006	max
$4^1(-1)^- \rightarrow 2^1 0^-$	13327 ± 75	0.0025 ± 0.0007	max
$4^1(-1)^- \rightarrow 3^1 0^-$	44050 ± 570	0.0027 ± 0.0009	max
$5^1(-1)^- \rightarrow 1^1 0^-$	4188 ± 16	0.0030 ± 0.0008	max
$5^1(-1)^- \rightarrow 2^1 0^-$	11292 ± 32	0.0035 ± 0.001	max
$5^1(-1)^- \rightarrow 3^1 0^-$	27640 ± 30	0.004 ± 0.001	max
$5^1(-1)^- \rightarrow 4^1 0^-$	48860 ± 280	0.195 ± 0.003	max
$5^1(-1)^- \rightarrow 4^1 0^-$	45700 ± 300	5.2 ± 0.2	min
$5^1(-1)^- \rightarrow 5^1 0^-$	98980 ± 600	0.0065 ± 0.0003	max
$5^1(-1)^- \rightarrow 5^1 0^-$	83470 ± 420	0.0221 ± 0.0009	min

Table 11: Same as Table 10 but for the triplet $|\Delta M| = 1$ within the subspace of negative z -parity, transitions $\mu^3(-1)^- \rightarrow \nu^3 0^-$ for $\mu = 1, \dots, 5$, $\nu = 1, \dots, 5$.

Component $\nu^{2S+1}M^{(-1)\Pi_z}$	wavelength/ \AA	position $B/a.u.$	max/min
$1^3(-1)^- \rightarrow 1^3 0^-$	7143 ± 30	0.1103 ± 0.0007	max
$2^3(-1)^- \rightarrow 1^3 0^-$	4574 ± 15	0.0087 ± 0.0003	max
$3^3(-1)^- \rightarrow 1^3 0^-$	4095 ± 10	0.0070 ± 0.0003	max
$3^3(-1)^- \rightarrow 2^3 0^-$	12680 ± 22	0.00965 ± 0.00006	max
$3^3(-1)^- \rightarrow 3^3 0^-$	51500 ± 1300	0.013 ± 0.001	max
$3^3(-1)^- \rightarrow 3^3 0^-$	43530 ± 400	0.046 ± 0.004	min
$4^3(-1)^- \rightarrow 1^3 0^-$	4063 ± 12	0.0024 ± 0.0003	max
$4^3(-1)^- \rightarrow 2^3 0^-$	12263 ± 25	0.00224 ± 0.00007	max
$4^3(-1)^- \rightarrow 3^3 0^-$	40265 ± 110	0.00264 ± 0.00001	max
$4^3(-1)^- \rightarrow 3^3 0^-$	23021 ± 40	0.079 ± 0.007	min
$4^3(-1)^- \rightarrow 3^3 0^-$	23532 ± 50	0.17 ± 0.01	max
$5^3(-1)^- \rightarrow 1^3 0^-$	3850 ± 9	0.0033 ± 0.0009	max
$5^3(-1)^- \rightarrow 2^3 0^-$	10505 ± 20	0.0035 ± 0.0007	max
$5^3(-1)^- \rightarrow 3^3 0^-$	26225 ± 70	0.0050 ± 0.0005	max
$5^3(-1)^- \rightarrow 4^3 0^-$	44662 ± 30	0.24 ± 0.02	max
$5^3(-1)^- \rightarrow 5^3 0^-$	91500 ± 1200	0.0062 ± 0.0003	max
$5^3(-1)^- \rightarrow 5^3 0^-$	2950 ± 530	0.022 ± 0.001	min

References

- [1] H. Friedrich, Phys.Rev. **A 26**, 1827 (1982)
- [2] W. Rösner, G. Wunner, H. Herold and H. Ruder, J.Phys. **B 17**, 29 (1984)
- [3] D. Wintgen and H. Friedrich, J.Phys. **B 19**, 991 (1986)
- [4] M.V. Ivanov, J.Phys. **B 21**, 447 (1988)
- [5] Yu.P. Kravchenko, M.A. Liberman and B. Johansson, Phys.Rev. **A 54**, 287 (1996)
- [6] H. Ruder, G. Wunner, H. Herold und F. Geyer, Atoms in Strong Magnetic Fields, Springer Verlag A-A 1994.
- [7] P. Schmelcher and W. Schweizer (Eds.), Atoms and Molecules in Strong External Fields, Plenum Press 1998
- [8] R.F. Green and J. Liebert, Pub. Astr. Soc. Pac 93, 105 (1980)
- [9] G.D. Schmidt, W.B. Latter, C.B. Foltz, Astrophysical Journal 350, 758 (1990)
- [10] G.D. Schmidt, R.G. Allen, P.S. Smith, J. Liebert, Astrophysical Journal 463, 320 (1996)
- [11] S. Jordan, P. Schmelcher, W. Becken and W. Schweizer, Astronomy & Astrophysics Letters **336**, L33-L36 (1998)
- [12] W. Becken, P. Schmelcher and F.K. Diakonov, J. Phys.**B 32**, 1557 (1999)
- [13] M.D. Jones and G. Ortiz, Phys.Rev. **A 59**, 2875 (1999)
- [14] A. Scrinzi, Phys.Rev. **A 58**, 3879 (1998)
- [15] V.B. Pavlov-Verevkin and B.I. Zhilinskii, Phys. Letters, **78A**, no. 3, 244 (1980)
- [16] G.W.F. Drake and Z.-C. Yan, Phys.Rev. **A 46** 2378 (1992)
- [17] D.M. Larsen, Phys.Rev. **B 20**, 20 (1979)
- [18] M.D. Jones, G. Ortiz, D.M. Ceperley, Phys.Rev. **A 54**, 219 (1996)
- [19] M.D. Jones, G. Ortiz, D.M. Ceperley, Phys.Rev. **E 55**, 6202 (1997)
- [20] M.V. Ivanov, J.Phys. **B 27**, 4513 (1994)
- [21] G. Thurner, H. Körbel, M. Braun, H. Herold, H. Ruder and G. Wunner, J.Phys. **B 26**, 4719 (1993)
- [22] K. Singer, Proc. R. Soc. Lond. **A 402**, 412 (1960)
- [23] I. S. Gradshteyn and I. M. Ryzhik, Table of integrals, series, and products, Academic Press, 1980
- [24] P. Appell et J. Kampé de Fériet, Les fonctions hypergéométriques et hypersphériques, Gauthier-Villars et Cie, Editeurs, Paris 1926
- [25] M. Abramowitz and I.A. Stegun, Handbook of mathematical functions, Dover Publications, 1972
- [26] W. Becken and P. Schmelcher, *submitted to Journal of Computational and Applied Mathematics*